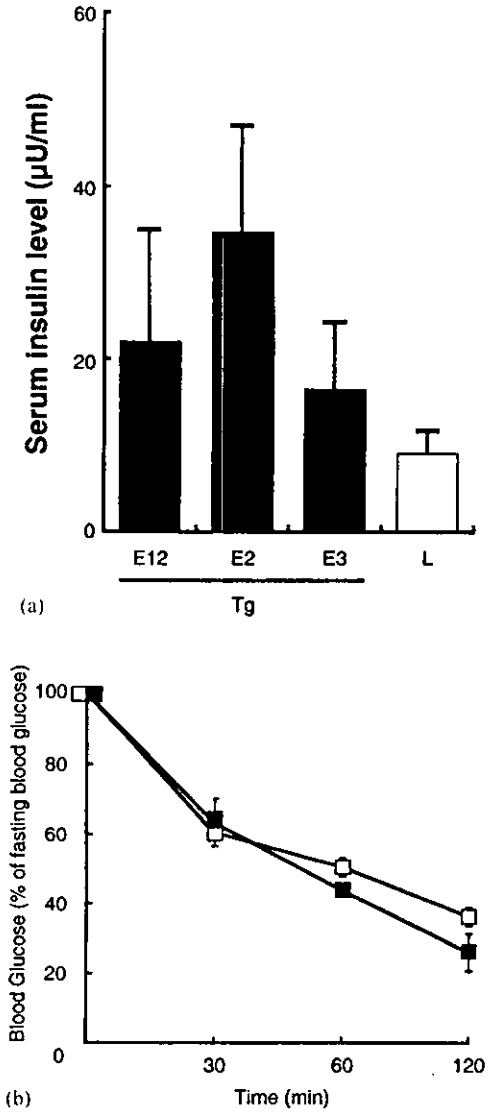

Fig. 6. Serum insulin levels and insulin tolerance test. (A) Measurement of insulin in EAT transgenic mice and non-transgenic mice. Three lines of transgenic mice were used for analysis. Of the 24 transgenic mice studied, 13 were from the E12 line (ages ranging from 8 to 22 months), 3 were from the E2 line (ages ranging from 19 to 24 months), and 8 were from the E3 line (ages ranging from 8 to 19 months). Thirty-three non-transgenic mice were studied (age 8 months). Mice were fasted overnight prior to intraperitoneal glucose administration (2 mg glucose/g BW). Blood was collected from the right cardiac ventricle 15 min after glucose administration. Error bars represent SEM. Tg, transgenic mice; non-Tg, non-transgenic mice. (B) Insulin tolerance test in EAT transgenic (open square) and non-transgenic (closed square) mice. Of the 8 mice from the E12 line studied, 4 were transgenic (age 8 months) and 4 were non-transgenic (ages ranging from 5 to 8 months). After overnight fasting, insulin (0.5 Units/kg BW) was injected into the peritoneal cavity of mice. Blood samples were collected from the tail at the indicated time and glucose concentrations were measured. Error bars represent SEM.

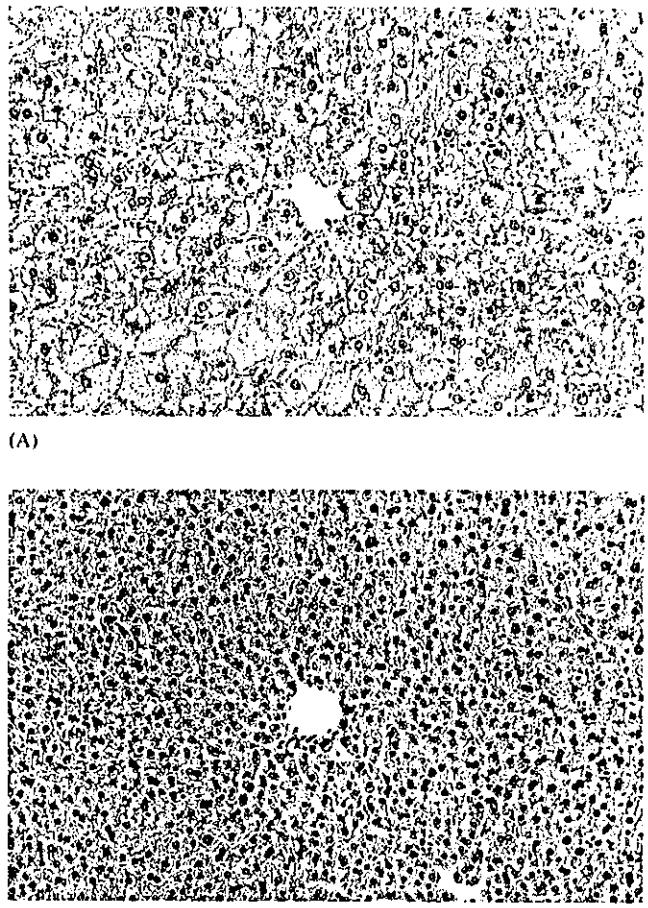

Fig. 7. Fatty metamorphosis of the liver in EAT transgenic mice. (A) Severe fatty metamorphosis was observed in the liver of transgenic mice in association with islet cell hyperplasia. (B) Normal appearance of hepatocytes in the non-transgenic liver. H&E staining. Original magnifications, × 100.

3.6. Islet cell adenoma in the EAT transgenic mouse

In addition to the above hyperplastic changes, we observed an extremely enlarged islet juxtaposed to hyperplastic islets in one EAT transgenic mouse (Fig. 8A). Histological analysis of this region revealed a coarse chromatin structure of the nuclei and prominent nucleoli compared with normal islets (Fig. 8B and C). In this enlarged islet region, all the cells were positive for insulin and there were no cells positive for glucagon (data not shown). Thus, this enlarged islet was considered to be an adenoma rather than a hyperplasia. This islet cell adenoma may have developed because of a second hit or mutation to certain genes governing the malignant transformation of cells.

4. Discussion

4.1. Mechanisms of islet cell hyperplasia in EAT transgenic mice

Apoptosis plays a key role in normal development and tissue homeostasis (Korsmeyer, 1995; Lewin and

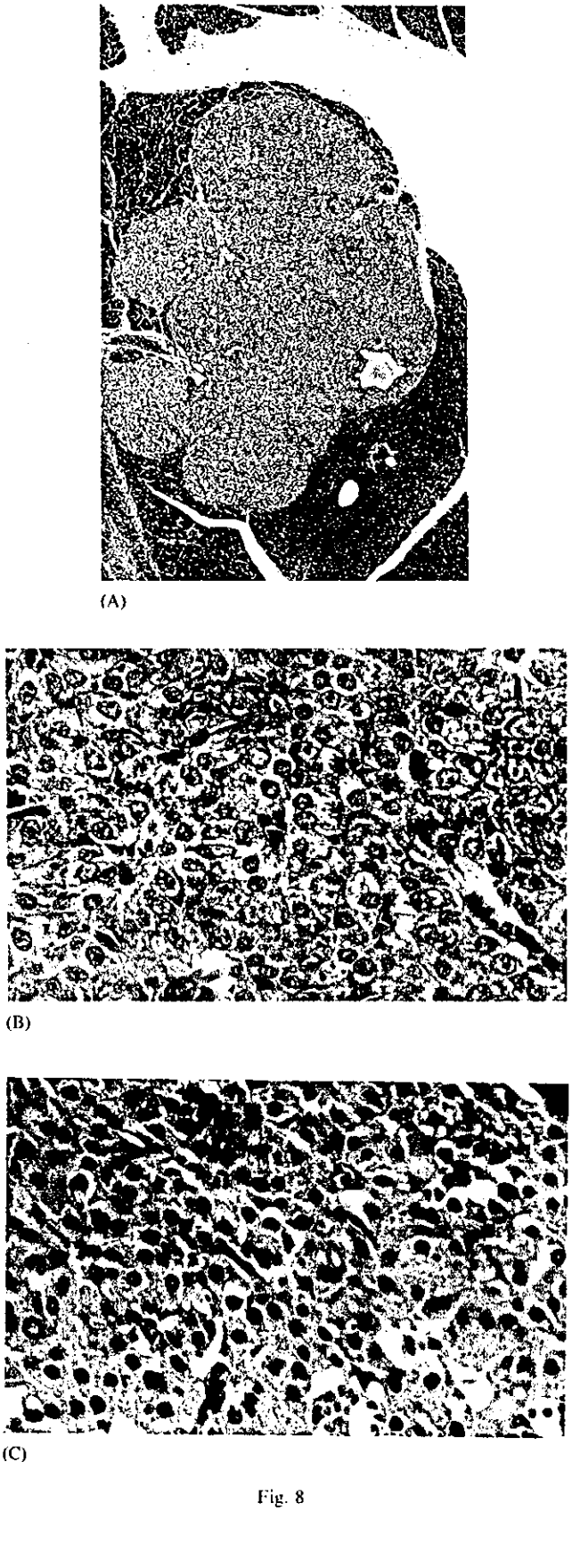

(A)

(B)

(C)

Fig. 8

Barde, 1996). β cells in the adult endocrine pancreas have been reported to have a life span of approximately 30 days, after which they undergo apoptosis (Finegood et al., 1995). The process of replication and proliferation in the pancreas—the neogenesis of new β cells derived from progenitor cells that bud from the ducts of the exocrine pancreas—allows for the replacement of these apoptotic β cells. Mathematical models have shown that though the replication rate of β cells in the adult rodent is only about 3% per day, the β-cell mass will double in 1 month if the apoptotic elimination of β cells are ignored (Finegood et al., 1995).

The EAT gene is considered to be a member of the bcl-2 related gene family based upon its possession of the BH domains 1, 2, 3 and 4 (Kroemer, 1997; Revilla et al., 1997). Similar to bcl-2, EAT has been shown to inhibit apoptosis in vitro (Reynolds et al., 1994; Sano et al., 2001). BH domains (BH1 to BH4) determine the capacity of bcl-2 related proteins to interact with each other or with other unrelated proteins. The ratio of death antagonists to agonists is known to determine whether a cell will undergo apoptosis. This death-life balance is regulated partly by competitive dimerization between pairs of antagonists and agonists (Kroemer, 1997). Up-regulation of Bax and Bag-1, both bcl-2 related genes, in EAT transgenic islets supports the hypothesis that EAT could inhibit apoptosis of pancreatic islet cells. Bax, which is known to be a pro-apoptotic molecule and heterodimeric partner for Bcl-2, was reported to display the same pattern of combinatorial interactions with EAT as Bcl-2 (Sedlak et al., 1995; Yang et al., 1995b). Similar to bcl-2, EAT may heterodimerize with Bax through BH1 and BH2 domains to repress apoptosis. Bag-1, an anti-apoptotic molecule, can interact with Bcl-2 and coexpression of BCL-2 and BAG-1 is more protective than expression of either protein alone (Schulz et al., 1997; Terada et al., 1997). Although Bag-1 has not been demonstrated to combine with EAT, Bag-1 may be a possible heterodimeric partner for EAT as it docks to the BH4 domain which EAT has been shown to possess (Kroemer, 1997).

The human bcl-2 gene has been shown to prevent cytokine-induced β-cell apoptosis in pancreatic islet cells (Iwahashi et al., 1996; Liu et al., 1996). Our results suggests that the protection afforded by EAT towards

Fig. 8. Islet cell adenoma in one EAT transgenic mouse. (A) An islet-cell adenoma was observed in one 16-month-old EAT transgenic mouse from the E12 line. H&E staining. Original magnifications, × 10. (B) Atypical nuclei are observed in the adenoma cells. Prominent nucleoli and a coarse chromatin pattern are observed in the adenoma cells. H&E staining. Original magnifications, × 400. (C) Normal appearance of pancreatic islet cells in a 12-month-old non-transgenic mouse from the E12 line. H&E staining. Original magnifications, × 400.

islet cell apoptosis led to islet cell hyperplasia in these transgenic mice.

4.2. Hyperplasia is observed with only the islets of the pancreas and is detected only after 4 months of age

The use of the EF1α promoter allows for ubiquitous tissue expression of the EAT transgene, yet hyperplastic changes were observed in only the pancreatic islets and not in other tissues. One possible mechanism may be that the expression level of the transgene was higher in pancreatic islets compared with other tissues. Another possible factor may be the lack of expression of genes which could block EAT function in the pancreatic islets. No bcl-2 related genes were detected in non-transgenic islets. Thus we would like to hypothesize that molecules which could block EAT function in the apoptotic pathway may not be expressed in the pancreatic islets and allow for this exaggerated effect of EAT in islet cells. In other words, the cellular environment in pancreatic islets may be suited for this EAT-induced hyperplasia (Cheatham and Kahn, 1995; Saltiel, 1996).

Hyperplasia was not observed in EAT transgenic mice before the age of 4 months. This may be due to the dynamics of islet cell growth based on the process of cell proliferation and apoptosis. During the neonatal period, approximately 10% of the fetal islet cells are undergoing apoptosis at any given point, but this fraction decreases to 3% in adult islets indicating that cell replication decreases after the neonatal period (Finegood et al., 1995). The fraction of apoptotic cells remains almost constant after the neonatal period. This ratio of cell proliferation to apoptosis is a critical determinant of total islet cell mass; while total islet cell and pancreatic mass increases dramatically due to the high proliferation rate before 4 months of age, the total mass maintains a stable balance after 4 months of age due to the relative decrease in this ratio of cell proliferation to apoptosis. Therefore, the influence of apoptosis on islet cell mass remains negligible before 4 months of age, but becomes a more significant factor after 4 months of age.

4.3. Differences among three transgenic lines

A difference in the incidence of islet cell hyperplasia was observed among the three transgenic lines. Fewer hyperplastic islets were observed in the E3 line as compared to the other two lines. This finding may suggest that the E3 line does not show any specific phenotype. This may be explained by three factors: expression level, copy number, and integration site. The phenotypes that we observed in the various lines were closely correlated with expression levels. The expression level of hEAT was found to be highest in the E2 line and to be lowest in the E3 line, though the difference between the E3 and E12 lines was subtle. In contrast, we found that the copy number of the transgene per diploid genome in the E3 line was higher compared with the other two lines; however, it is known that expression level is independent of copy number. We were not able to correlate our phenotypes with the integration sites, and find it difficult to forward a precise explanation for this; nevertheless, gene induction is known to be stochastic (Ko, 1992; Ko et al., 1990b) and variability of results is commonly observed with the transgenic approach.

4.4. Clinical impact of the anti-apoptotic activities of EAT in β cells

Our results suggest that EAT may play a role in the inhibition of pancreatic β cells from apoptosis in vivo. Apoptosis of β cells is considered to be a prevalent mechanism in insulin-dependent diabetes mellitus (IDDM) (Rossini et al., 1993), a T-cell mediated autoimmune disease (McInerney et al., 1996; Wong and Janeway, 1997). Although the precise role of apoptosis in β cell destruction in IDDM remains to be defined, both soluble mediators and Fas antigen may possibly be involved (Chervonsky et al., 1997; Itoh et al., 1993). Cytotoxic T cells can induce apoptosis of β cells via the Fas pathway, and overexpression of bcl-2 has been reported to inhibit this Fas-induced cell death (Itoh et al., 1993). The possession of anti-apoptotic activity by EAT towards β cells, shown in this investigation, suggests the use of EAT under certain conditions to inhibit or delay apoptosis of β cells. Establishment of EAT inhibition of β cell apoptosis in humans, hints at possible future genetic therapies for IDDM.

Acknowledgements

We are grateful to J. Ozawa, K. Otsuki, H. Suzuki, S. Kusakari, H. Abe, Y. Hashimoto and M. Takahashi for their technical assistance and K. Takeichi for photographic assistance. We also thank to T. Ando, H. Kikuchi, T. Atsumi, and A. Hashiguchi for useful discussion. This work was supported in part by a grant from the Ministry of Education, Science and Culture to J.H. and A.U., by Keio University Special Grant-in-Aid for Innovative Collaborative Research Project to J.H. and A.U., by Keio Gijuku Fukuzawa Memorial Funds for the Advancement of Education and Research from Keio University to H.O., and by a National Grant-in-Aid for the Establishment of a High-Tech Research Center at Private Universities.

References

Adams, J.M., Cory, S., 1998. The Bcl-2 protein family: arbiters of cell survival. Science 281, 1322–1326.

Akgul, C., Moulding, D.A., White, M.R., Edwards, S.W., 2000a. In vivo localisation and stability of human Mcl-1 using green fluorescent protein (GFP) fusion proteins. FEBS Lett. 478, 72–76.

Akgul, C., Turner, P.C., White, M.R., Edwards, S.W., 2000b. Functional analysis of the human MCL-1 gene. Cell Mol. Life Sci. 57, 684–691.

Ando, T., Umezawa, A., Suzuki, A., Okita, H., Sano, M., Hiraoka, Y., Aiso, S., Saruta, T., Hata, J., 1998. EAT/mcl-1, a member of the bcl-2 related genes, confers resistance to apoptosis induced by cis-diammine dichloroplatinum (II) via a p53- independent pathway. Jpn J. Cancer Res. 89, 1326–1333.

Bingle, C.D., Craig, R.W., Swales, B.M., Singleton, V., Zhou, P., Whyte, M.K., 2000. Exon skipping in Mcl-1 results in a bcl-2 homology domain 3 only gene product that promotes cell death. J. Biol. Chem. 275, 22136–22146.

Boise, L.H., Gonzalez-Garcia, M., Postema, C.E., Ding, L., Lindsten, T., Turka, L.A., Mao, X., Nunez, G., Thompson, C.B., 1993. bcl-x, a bcl-2-related gene that functions as a dominant regulator of apoptotic cell death. Cell 74, 597–608.

Brady, H.J., Gil-Gomez, G., Kirberg, J., Berns, A.J., 1996a. Bax alpha perturbs T cell development and affects cell cycle entry of T cells. EMBO J. 15, 6991–7001.

Brady, H.J., Salomons, G.S., Bobeldijk, R.C., Berns, A.J., 1996b. T cells from baxalpha transgenic mice show accelerated apoptosis in response to stimuli but do not show restored DNA damage-induced cell death in the absence of p53 gene product in. EMBO J. 15, 1221–1230.

Chao, D.T., Korsmeyer, S.J., 1998. BCL-2 family: regulators of cell death. Annu. Rev. Immunol. 16, 395–419.

Cheatham, B., Kahn, C.R., 1995. Insulin action and the insulin signaling network. Endocr. Rev. 16, 117–142.

Chervonsky, A.V., Wang, Y., Wong, F.S., Visintin, I., Flavell, R.A., Janeway, C., Jr., Matis, L.A., 1997. The role of Fas in autoimmune diabetes. Cell 89, 17–24.

Chittenden, T., Harrington, E.A., O'Connor, R., Flemington, C., Lutz, R.J., Evan, G.I., Guild, B.C., 1995. Induction of apoptosis by the Bcl-2 homologue Bak. Nature 374, 733–736.

D'Sa-Eipper, C., Subramanian, T., Chinnadurai, G., 1996. bfl-1, a bcl-2 homologue, suppresses p53-induced apoptosis and exhibits potent cooperative transforming activity. Cancer Res. 56, 3879–3882.

Finegood, D.T., Scaglia, L., Bonner-Weir, S., 1995. Dynamics of beta-cell mass in the growing rat pancreas. Estimation with a simple mathematical model. Diabetes 44, 249–256.

Gibson, L., Holmgreen, S.P., Huang, D.C., Bernard, O., Copeland, N.G., Jenkins, N.A., Sutherland, G.R., Baker, E., Adams, J.M., Cory, S., 1996. bcl-w, a novel member of the bcl-2 family, promotes cell survival. Oncogene 13, 665–675.

Gotoh, M., Maki, T., Kiyoizumi, T., Satomi, S., Monaco, A.P., 1985. An improved method for isolation of mouse pancreatic islets. Transplantation 40, 437–438.

Hanaoka, K., Hayasaka, M., Uetsuki, T., Fujisawa-Sehara, A., Nabeshima, Y., 1991. A stable cellular marker for the analysis of mouse chimeras: the bacterial chloramphenichol acetyltransferase driven by the human elongation factor 1a promoter. Differentiation 48, 183–189.

Hata, J.-I., Fujimoto, J., Ishii, E., Umezawa, A., Kokai, Y., Matsubayashi, Y., Abe, H., Kusakari, S., Kikuchi, H., Yamada, T., Maruyama, T., 1992. Differentiation of human germ cell tumor cells in vivo and in vitro. Acta Histochem. Cytochem. 25, 563–576.

Hogan, B., Constantini, F., Howard, B.H., 1986. Manipulating The Mouse Embryo. Cold Spring Harbor Laboratory Press, New York.

Inohara, N., Ding, L., Chen, S., Nunez, G., 1997. Harakiri, a novel regulator of cell death, encodes a protein that activates apoptosis and interacts selectively with survival-promoting proteins Bcl-2 and Bcl-X(L). EMBO J. 16, 1686–1694.

Itoh, N., Tsujimoto, Y., Nagata, S., 1993. Effect of bcl-2 on Fas antigen-mediated cell death. J. Immunol. 151, 621–627.

Iwahashi, H., Hanafusa, T., Eguchi, Y., Nakajima, H., Miyagawa, J., Itoh, N., Tomita, K., Namba, M., Kuwajima, M., Noguchi, T., Tsujimoto, Y., Matsuzawa, Y., 1996. Cytokine-induced apoptotic cell death in a mouse pancreatic beta-cell line: inhibition by Bcl-2. Diabetologia 39, 530–536.

Knudson, C.M., Tung, K.S., Tourtellotte, W.G., Brown, G.A., Korsmeyer, S.J., 1995. Bax-deficient mice with lymphoid hyperplasia and male germ cell death. Science 270, 96–99.

Ko, M.S., 1992. Induction mechanism of a single gene molecule: stochastic or deterministic? Bioessays 14, 341–346.

Ko, M.S., Ko, S.B., Takahashi, N., Nishiguchi, K., Abe, K., 1990a. Unbiased amplification of a highly complex mixture of DNA fragments by 'lone linker'-tagged PCR. Nucleic Acids Res. 18, 4293–4294.

Ko, M.S., Nakauchi, H., Takahashi, N., 1990b. The dose dependence of glucocorticoid-inducible gene expression results from changes in the number of transcriptionally active templates. EMBO J. 9, 2835–2842.

Korsmeyer, S.J., 1995. Regulators of cell death. Trends. Genet. 11, 101–105.

Kozopas, K.M., Yang, T., Buchan, H.L., Zhou, P., Craig, R.W., 1993. MCL1, a gene expressed in programmed myeloid cell differentiation, has sequence similarity to BCL2. Proc. Natl. Acad. Sci. USA 90, 3516–3520.

Kroemer, G., 1997. The proto-oncogene Bcl-2 and its role in regulating apoptosis. Nat. Med. 3, 614–620.

Lacy, P.E., Kostianovsky, M., 1967. Method for the isolation of intact islets of Langerhans from the rat pancreas. Diabetes 16, 35–39.

Lewin, G.R., Barde, Y.A., 1996. Physiology of the neurotrophins. Annu. Rev. Neurosci. 19, 289–317.

Lin, E.Y., Orlofsky, A., Wang, H.G., Reed, J.C., Prystowsky, M.B., 1996. A1, a Bcl-2 family member, prolongs cell survival and permits myeloid differentiation. Blood 87, 983–992.

Liu, Y., Rabinovitch, A., Suarez-Pinzon, W., Muhkerjee, B., Brownlee, M., Edelstein, D., Federoff, H.J., 1996. Expression of the bcl-2 gene from a defective HSV-1 amplicon vector protects pancreatic beta-cells from apoptosis. Hum. Gene Ther. 7, 1719–1726.

Matsushita, K., Umezawa, A., Iwanaga, S., Oda, T., Okita, H., Kimura, K., Shimada, M., Tanaka, M., Sano, M., Ogawa, S., Hata, J., 1999. The EAT/mcl-1 gene, an inhibitor of apoptosis, is up-regulated in the early stage of acute myocardial infarction. Biochim. Biophys. Acta 1472, 471–478.

McDonnell, T.J., Deane, N., Platt, F.M., Nunez, G., Jaeger, U., McKearn, J.P., Korsmeyer, S.J., 1989. bcl-2-immunoglobulin transgenic mice demonstrate extended B cell survival and follicular lymphoproliferation. Cell 57, 79–88.

McInerney, M.F., Flynn, J.C., Goldblatt, P.J., Najjar, S.M., Sherwin, R.S., Janeway, C., Jr., 1996. High density insulin receptor-positive T lymphocytes from nonobese diabetic mice transfer insulitis and diabetes. J. Immunol. 157, 3716–3726.

Moulding, D.A., Giles, R.V., Spiller, D.G., White, M.R., Tidd, D.M., Edwards, S.W., 2000. Apoptosis is rapidly triggered by antisense depletion of MCL-1 in differentiating U937 cells. Blood 96, 1756–1763.

Okita, H., Umezawa, A., Suzuki, A., Hata, J., 1998. Up-regulated expression of murine Mcl1/EAT, a bcl-2 related gene, in the early stage of differentiation of murine embryonal carcinoma cells and embryonic stem cells. Biochim. Biophys. Acta 1398, 335–341.

Reed, J.C., 1998. Bcl-2 family proteins. Oncogene 17, 3225–3236.

Revilla, Y., Cebrian, A., Baixeras, E., Martinez, C., Vinuela, E., Salas, M.L., 1997. Inhibition of apoptosis by the African swine fever

virus Bcl-2 homologue: role of the BH1 domain. Virology 228, 400–404.

Reynolds, J.E., Yang, T., Qian, L., Jenkinson, J.D., Zhou, P., Eastman, A., Craig, R.W., 1994. Mcl-1, a member of the Bcl-2 family, delays apoptosis induced by c-Myc overexpression in Chinese hamster ovary cells. Cancer Res. 54, 6348–6352.

Rossini, A.A., Greiner, D.L., Friedman, H.P., Mordes, J.P., 1993. Immunopathogenesis of diabetes mellitus. Diabetes Rev. 1, 43–75.

Saltiel, A.R., 1996. Diverse signaling pathways in the cellular actions of insulin. Am. J. Physiol. 270, E375–E385.

Sano, M., Umezawa, A., Abe, H., Akatsuka, A., Nonaka, S., Shimizu, H., Fukuma, M., Hata, J., 2001. EAT/mcl-1 expression in the human embryonal carcinoma cells undergoing differentiation or apoptosis. Exp. Cell Res. 266, 114–125.

Sano, M., Umezawa, A., Suzuki, A., Shimoda, K., Fukuma, M., Hata, J., 2000. Involvement of EAT/mcl-1, an anti-apoptotic bcl-2-related gene, in murine embryogenesis and human development. Exp. Cell Res. 259, 127–139.

Schulz, J.B., Bremen, D., Reed, J.C., Lommatzsch, J., Takayama, S., Wullner, U., Loschmann, P.A., Klockgether, T., Weller, M., 1997. Cooperative interception of neuronal apoptosis by BCL-2 and BAG-1 expression: prevention of caspase activation and reduced production of reactive oxygen species. J. Neurochem. 69, 2075–2086.

Sedlak, T.W., Oltvai, Z.N., Yang, E., Wang, K., Boise, L.H., Thompson, C.B., Korsmeyer, S.J., 1995. Multiple Bcl-2 family members demonstrate selective dimerizations with Bax. Proc. Natl. Acad. Sci. USA 92, 7834–7838.

Sentman, C.L., Shutter, J.R., Hockenbery, D., Kanagawa, O., Korsmeyer, S.J., 1991. bcl-2 inhibits multiple forms of apoptosis but not negative selection in thymocytes. Cell 67, 879–888.

Siegel, R.M., Katsumata, M., Miyashita, T., Louie, D.C., Greene, M.I., Reed, J.C., 1992. Inhibition of thymocyte apoptosis and negative antigenic selection in bcl-2 transgenic mice. Proc. Natl. Acad. Sci. USA 89, 7003–7007.

Strasser, A., Harris, A.W., Cory, S., 1991. bcl-2 transgene inhibits T cell death and perturbs thymic self-censorship. Cell 67, 889–899.

Terada, S., Fukuoka, K., Fujita, T., Komatsu, T., Takayama, S., Reed, J.C., Suzuki, E., 1997. Anti-apoptotic genes, bag-1 and bcl-2, enabled hybridoma cells to survive under treatment for arresting cell cycle. Cytotechnology 25, 17–23.

Umezawa, A., Maruyama, T., Inazawa, J., Imai, S., Takano, T., Hata, J., 1996. Induction of mcl1/EAT, Bcl-2 related gene, by retinoic acid or heat shock in the human embryonal carcinoma cells, NCR-G3. Cell Struct. Funct. 21, 143–150.

Veis, D.J., Sorenson, C.M., Shutter, J.R., Korsmeyer, S.J., 1993. Bcl-2-deficient mice demonstrate fulminant lymphoid apoptosis, polycystic kidneys, and hypopigmented hair. Cell 75, 229–240.

Wang, K., Yin, X.M., Chao, D.T., Milliman, C.L., Korsmeyer, S.J., 1996. BID: a novel BH3 domain-only death agonist. Genes Dev. 10, 2859–2869.

Wong, F.S., Janeway, C., Jr., 1997. The role of CD4 and CD8 T cells in type 1 diabetes in the NOD mouse. Res. Immunol. 148, 327–332.

Yang, E., Zha, J., Jockel, J., Boise, L.H., Thompson, C.B., Korsmeyer, S.J., 1995a. Bad, a heterodimeric partner for Bcl-XL and Bcl-2, displaces Bax and promotes cell death. Cell 80, 285–291.

Yang, T., Kozopas, K.M., Craig, R.W., 1995b. The intracellular distribution and pattern of expression of Mcl-1 overlap with, but are not identical to, those of Bcl-2. J. Cell Biol. 128, 1173–1184.

J Periodont Res 2003; 38; 333–342
Printed in the UK. All rights reserved

JOURNAL OF PERIODONTAL RESEARCH
ISSN 0022-3484

The effects of enamel matrix derivative (EMD) on osteoblastic cells in culture and bone regeneration in a rat skull defect

Satoshi Yoneda[1], Daisuke Itoh[1], Shinji Kuroda[1], Hisatomo Kondo[1], Akihiro Umezawa[2], Keiichi Ohya[3], Takashi Ohyama[4], Shohei Kasugai[1]

[1]Masticatory Function Control, Tokyo Medical and Dental University, [2]Pathology, Keio University School of Medicine, [3]Pharmacology, Hard Tissue Engineering, Tokyo Medical and Dental University, [4]Removable Prosthodontics, Tokyo Medical and Dental University, Tokyo, Japan

Yoneda S, Itoh D, Kuroda S, Kondo H, Umezawa A, Ohya K, Ohyama T, Kasugai S. The effects of enamel matrix derivative (EMD) on osteoblastic cells in culture and bone regeneration in a rat skull defect. J Periodont Res 2003; 38; 333–342. © Blackwell Munksgaard, 2003

Objective: Enamel matrix derivative (EMD) has been clinically used to promote periodontal tissue regeneration. The purpose of the present study is to clarify EMD affects on osteoblastic cells and bone regeneration.

Materials and Methods: Mouse osteoblastic cells (ST2 cells and KUSA/A1 cells) are used in culture experiments. After cells were treated with EMD, cell growth was evaluated with DNA measurement, 5-bromo-2′-deoxyurydine (BrdU) incorporation assay. Measurement of alkaline phosphatase (ALP) activity and mineralized-nodule (MN) formation, Northern blotting analysis and zymography are also performed. In addition, EMD was applied to a rat skull defect and the defect was radiographically and histologically evaluated 2 weeks after the application.

Results: EMD did not stimulate ST2 cell growth; however, it enhanced KUSA/A1 cell proliferation. Although EMD stimulated ALP activity in both the cells, ALP activity in KUSA/A1 cells was affected to a much greater degree. Corresponding to the increase in ALP activity, MN formation in KUSA/A1 cells was enhanced by EMD. EMD stimulated osteoblastic phenotype expression of KUSA/A1 cells such as type I collagen, osteopontin, transforming growth factor beta 1 and osteocalcin. EMD treatment also stimulated matrix metalloproteinase production in KUSA/A1 cells. Although the effects of EMD on osteoblastic cells depend on cell type, the overall effect of EMD on osteoblastic cells is stimulatory rather than inhibitory. Finally, EMD application to a rat skull defect accelerated new bone formation.

Conclusion: These results indicate that EMD affects osteoblastic cells and has potential as a therapeutic material for bone healing.

Satoshi Yoneda, DDS, Masticatory Function Control, Tokyo Medical and Dental University, 1-5-45, Yushima, Bunkyo-ku, Tokyo, 113-8549, Japan
Tel: +81 3 5803 4554
Fax: +81 3 5803 5934
e-mail: kome.mfc@tmd.ac.jp

Key words: enamel matrix derivative; osteoblasts; culture; skull defect

Accepted for publication October 28, 2002

The implication of enamel matrix in cementogenesis in tooth development was suggested more than 20 years ago (1). In 1997, Hammarström (2) reported the formation of acellular cementum after experimentally exposing dental follicles [the progenitors of cementum, periodontal ligament (PDL) and alveolar bone] to enamel matrix. Furthermore, he and his collaborators (3, 4) demonstrated that enamel matrix derivative induces the formation of acellular cementum on denuded root surfaces in monkeys and humans. Thus, it is a logical choice to use enamel matrix derivative for periodontal tissue regeneration. EMD, in acid-extracted porcine

enamel derivative form, is commercially available.

Animal experiments (5–7) and clinical studies (8–12) have already demonstrated that EMD stimulates regeneration of periodontal tissue, including acellular cementum, PDL and alveolar bone. The effects of EMD on PDL cells in culture have been examined. EMD stimulates cellular proliferation, migration, alkaline phosphatase (ALP) activity, mineralized nodule (MN) formation, and transforming growth factor beta 1 (TGF-β1) production (13–15). These EMD effects on PDL cells could favorably contribute to periodontal tissue regeneration.

It has been reported that EMD affects osteoblastic cells *in vitro* (16, 17), and its effects depend on cell type; however, the precise effect of EMD on osteoblastic cells needs to be elucidated. In the present study, we used two mouse osteoblastic cell lines, ST2 and KUSA/A1 cells. ST2 cells can differentiate to the adipocyte and osteoblast. Although their osteoblastic differentiation and maturation are induced and stimulated by ascorbic acid, osteoblastic differentiation of ST2 cells needs a long period (18). On the other hand, KUSA/A1 cells have the ability to differentiate to osteoblast and they can form bone-like tissue early both *in vitro* and *in vivo* (19). Compared with ST2 cells, KUSA/A1 cells are highly committed to osteoblastic linage. To examine the effect of EMD on the osteoblastic differentiation and maturation, the following analyses were performed *in vitro*: cellular proliferation, ALP activity, MN formation, matrix metalloproteinase (MMP) production and mRNA expression of osteoblastic phenotypes.

The effect of EMD on bone *in vivo* has been reported: EMD enhances bone formation induced by bone morphogenetic protein (BMP) (20) and it stimulates bone regeneration of rat femurs (21). BMP-induced bone formation usually follows endochondral ossification and it is unlikely that bone regeneration of femur is similar to the one of oral-maxillofacial bones. Thus, in the present study, we used calvarial bone defect model to evaluate EMD effect on bone regeneration.

Materials and methods

EMD treatment and cell culture

EMD (Biora, Malmö, Sweden) was dissolved in 10 mM acetic acid and stored at −70°C. Before cell inoculation, a serum-free culture medium was added to the culture plates. Various concentrations of EMD (from 12.5 to 50 μg/ml) were added and the culture plates were incubated in a CO_2 incubator for 3 h. EMD precipitated and a fine deposition of EMD covered the bottom of the plates. This treatment did not affect the medium's pH. Two mouse osteoblastic cell lines, ST2 cells and KUSA/A1 cells, were used. ST2 cells were purchased from RIKEN Cell Bank (Saitama, Japan); KUSA/A1 cells were established by Umezawa (19), one of the authors. These cells were suspended in medium containing 20% FBS, and then inoculated onto plates that contained serum-free medium with EMD. The final concentration of FBS in the medium was 10%. After 24 h, the medium was aspirated without removing the precipitated EMD, and new culture medium was added to the plates. In all the experiments except the proliferation assays and ALP activity measurement, the culture medium was α-MEM (minimum essential medium alpha medium, GIBCO, Tulsa, OK, USA) supplemented with 10% fetal bovine serum (FBS: Lot no. 6H2167, Summit, Collins, CO, USA), 60 μg/ml kanamycin and 0.2 mM L-ascorbic acid phosphate magnesium salt (Wako Chemical Co., Osaka, Japan). The culture medium for KUSA/A1 cells was additionally supplemented with 5 mM β-glycerophosphate disodium salt (Sigma Chemical Co., St. Louis, MO, USA). The culture was maintained at 37°C in a humidified atmosphere consisting of 95% air and 5% CO_2.

Proliferation assays (DNA measurement and BrdU incorporation)

In proliferation assay experiments, FBS concentration in the culture medium was 5%. Ninety-six-well plates and 24-well plates were treated with EMD as described above. For DNA measurement, ST2 cells and KUSA/A1 cells were inoculated in 24-well plates at a cell density of 10^4 cells/cm^2 and 10^3 cells/cm^2, respectively. ST2 cells and KUSA/A1 cells were rinsed with Ca^{2+}-, Mg^{2+}-free phosphate buffered saline [PBS (−)], scraped into 0.3 ml of 0.9% NaCl containing 0.1% sodium dodecyl sulfate (SDS), and then homogenized using a sonicator (Sonicator 5202, Otake, Japan) on ice after 10 and 16 d, respectively. DNA content was spectrofluorometrically determined by the method reported by Labarca (22). Fifty microliters of the sample was mixed with Hoechst 33258 buffer (1 μg/ml Hoechst 33258, 0.05 M Na_3PO_4, 2.0 M NaCl, and 2.0 mM EDTA, pH 7.4). The fluorescence was read at 356 nm excitation and 458 nm emission using a spectrofluorometer (FP-777, JASCO, Japan). Salmon sperm DNA was used as the standard.

For the 5-bromo-2′-deoxyuridine (BrdU) incorporation assay, KUSA/A1 cells were inoculated into 96-well plates at a cell density of 10^3 cells/cm^2 and cultured. A BrdU incorporation assay (Amersham Pharmacia Biotech, UK) was performed at d 4, 8 and 14, following the manufacturer's instructions. In brief, the cells were labeled with BrdU for 24 h. The pyrimidine analogue BrdU was incorporated instead of thymidine into the DNA of proliferating cells (23) and incorporated BrdU was detected by means of enzyme-linked immunosorbent assay. The absorbance of resultant color was read at 450 nm in a microtitre plate spectrophotometer (Microplate Reader, Model 450, Bio-Rad).

Measurement of ALP activity

The activity of ALP was measured in both ST2 and KUSA/A1 cells. The sample was the same as the one used for DNA measurement and prepared as described above. In the culture of ST2 cells, ascorbic acid induces osteoblastic differentiation and maturation, which are detectable by an increase in ALP activity (18). Thus, medium with or without supplementation of ascorbic acid was used to examine the effects of EMD at various

differentiation stages of ST2 cells. ALP activity was measured using an ALP B-test Wako kit (Wako Chemical Co., Osaka, Japan) based on the method of Lowry-Bessey (24). Fifty microliters of the cell homogenate, part of the sample prepared for DNA measurement, was incubated with the assay buffer at 37°C and the solution was spectrophotometrically measured at 405 nm.

Measurement of mineralized nodule (MN) formation

Twenty-four-well plates were treated with EMD as described above. KUSA/A1 cells were inoculated into 24-well plates at a cell density of 5×10^3 cells/cm^2 and cultured. On d 10, the cultures were fixed with methanol and stained with Alizarin Red S. The stained image was acquired with a densitometor (GS-670, Bio-Rad) and analyzed for MN area by NIH Image 1.61 (National Institutes of Health, Bethesda, MD, USA) on a Macintosh computer.

Gelatin zymography

Substrate gel electrophoresis (zymography) was performed to identify the effect of EMD on the MMP production of KUSA/A1 cells. Culture dishes (35 mm) were treated with EMD as described above. KUSA/A1 cells were inoculated at a cell density of 5×10^3 cells/cm^2, and cultured. On d 4 and 7, KUSA/A1 cells were washed three times with PBS (–), and cultured in serum-free α-MEM for 24 h. The conditioned media was then collected and centrifuged at $1500 \times g$ for 5 min. All supernatants were diluted in a non-reducing sodium dodecyl sulfate-polyacrylamide gel electrophoresis (SDS-PAGE) buffer. The volume of each sample applied to the gel was adjusted depending on the number of cells, which was counted in the corresponding plate after trypsin treatment. The samples were electrophoresed on 15% SDS-polyacrylamide gels containing 2 mg/ml gelatin under non-reducing conditions. After electrophoresis, the gels were washed twice with 2.5% Triton X-100 for 1 h and then incubated in 50 mM Tris-HCl, pH 7.5 containing 5 mM $CaCl_2$, 0.02% NaN_3, 200 nM NaCl and 1 μM $ZnCl_2$ overnight at 37°C. The gels were stained with Coomassie Brilliant Blue R-250. This was followed by destaining.

Northern blot analysis

KUSA/A1 cells were inoculated onto 100-mm dishes treated with EMD, at a cell density of 5×10^3 cells/cm^2 and cultured. On d 4, 7 and 10, the total RNA of the cultures was extracted using an RNA extraction solution (RNAzol B, Biotecx Laboratories, TX, USA), which is based on the guanidine phenol/chloroform method (25). For Northern analysis, 10 μg of each total RNA was electrophoresed on 1.2% agarose gels, stained with ethidium bromide and transferred to nylon membranes (Zeta-Probe, Bio-Rad, CA, USA), using the capillary elution method. After prehybridization, hybridization with [^{32}P]-labeled cDNA was carried out overnight at 42°C. The following cDNA probes were used: a 900-base pair *Pst*I fragment of pα2R2 (α2 chain of rat type I collagen, COL I) (26); a 984-base pair *Hin*dIII fragment of mouse 2ar (osteopontin, OPN) (27); a 912-base pair of rat bone sialoprotein (BSP) (28); a 488-base pair *Eco*RI–*Pst*I fragment of mouse osteocalcin (OC) (29); cDNA of TGF-β1, nucleotide position from 693 to 1217 (30), was prepared by reverse transcription-polymerase chain reaction technique (RT-PCR) from mouse bone mRNA. This DNA fragment was inserted into a pBluescript SK (+) (Strategene Cloning Systems, La Jolla, CA, USA). The hybridized membranes were exposed to Kodak X-OMAT films.

In vivo activity

Twelve-week-old male Wistar rats were anesthetized by intramuscular injection of pentobarbital. An incision was made into the soft tissue, including the periosteum, and the bone surface was exposed. Full-thickness trephine defects (3.8 mm diameter) were created in the bilateral parietal bone. A lyophilized pellet, a 100 μl of 1% bovine atelocollagen (KOKEN Co., Tokyo, Japan) with or without 1 mg EMD, was inserted into the skull defect on the experimental (right-hand) side. The left side skull defect (control) was not filled. Furthermore, to examine the possibility of the involvement of EMD in ectopic bone formation, a pellet of each type was also placed into the hind thigh muscle. Four animals were used for each group described above. Two weeks after the surgical operation, the rats were sacrificed, and the tissues around the operation site were taken and fixed with 10% buffered formalin. To evaluate new bone formation, soft X-ray photographs were taken. Photographic images were acquired with a densitometor (GS-670, Bio-Rad) and analyzed with NIH image 1.61 software on a Macintosh computer. The samples were embedded in methyl methacrylate resin, and ground sections containing the central region of the bone defect were prepared and stained with toluidine blue.

Statistical methods

Numerical data were presented as mean plus one standard deviation. One way analysis of variance (ANOVA) with Fisher's PLSD test was used for multiple comparisons to compare with the control. The probability level of $P < 0.05$ was regarded as statistically significant.

Results

Cell proliferation

In DNA measurements, EMD did not affect ST2 cell growth (data not shown), whereas it stimulated KUSA/A1 cell growth in a concentration-dependent manner (Fig. 1A). When KUSA/A1 cells were inoculated at a cell density of 10^3 cells/cm^2, the cells reached the confluent stage at d 6. The stimulatory effect of EMD on KUSA/A1 cell proliferation was also revealed in the BrdU incorporation assay. These stimulatory effects were observed within 20 days. As shown in Fig. 1(B), EMD stimulated the proliferation of KUSA/A1 cells in a concentration-dependent manner at three different time points: d 4, 8 and 14.

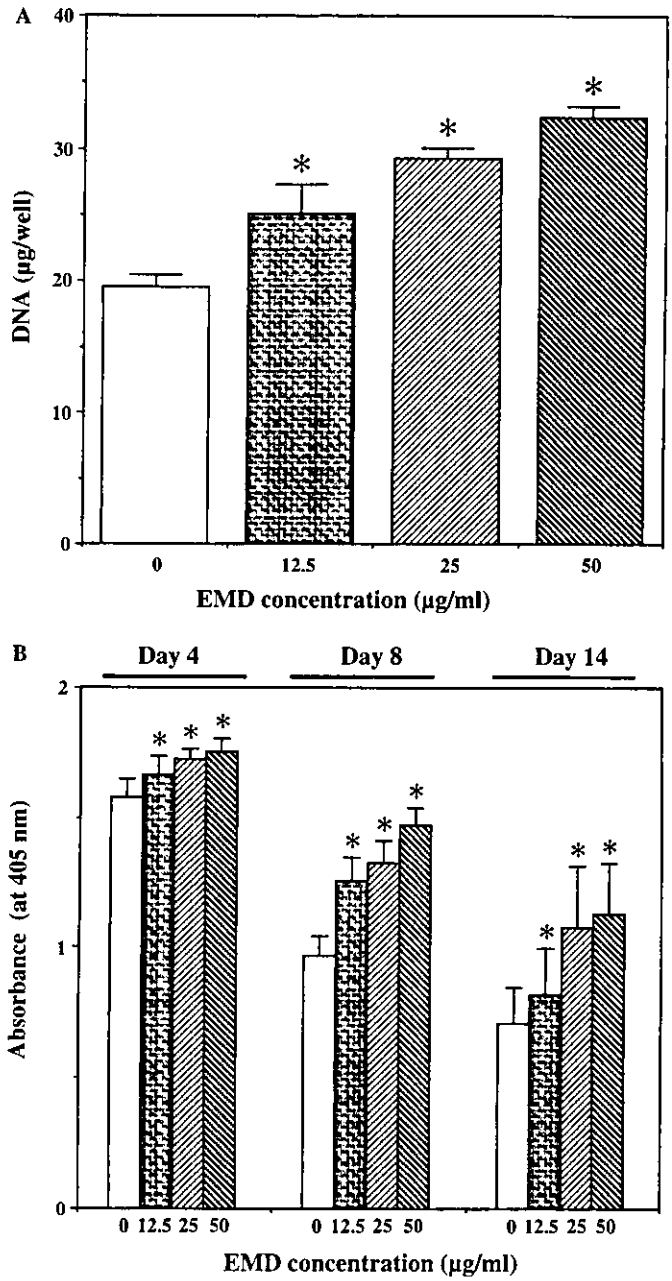

Fig. 1. Effect of EMD on proliferation of KUSA/A1 cells. KUSA/A1 cells were cultured in various concentrations of EMD. Cellular proliferation was analyzed by DNA measurement at d 10 (A) and by BrdU incorporation at d 4, 8 and 14 (B). Data are presented as the mean + SD. $n = 4$ (A) and $n = 6$ (B). *Significantly different from the control at $P < 0.05$.

ALP activity

In ST2 cells, ALP activity was stimulated by EMD in a concentration-dependent manner when culture medium was supplemented with ascorbic acid (Fig. 2A). However, when the culture medium was not supplemented with ascorbic acid, ALP activity of ST2 cells was relatively low, and the EMD stimulatory effect on ALP activity was not observed under this culture condition. In KUSA/A1 cells, EMD stimulated ALP activity in a concentration-dependent manner (Fig. 2B).

MN formation

EMD stimulated MN area of KUSA/A1 cells in a concentration-dependent manner (Fig. 3). Under phase contrast microscopy, the morphology of KUSA/A1 cells was fibroblastic and gradually grew into multiple layers of cells (data not shown). Part of the cell layer became dense and started to mineralize at d 9 or 10. In the EMD-treated culture of KUSA/A1 cells, a thick cell layer with matrix accumulation was evident compared to the control culture.

MMP activity

After the KUSA/A1 cells had been treated with EMD, aliquots of conditioned medium were electrophoresed on SDS-polyacrylamide gels containing gelatin. As shown in Fig. 4, proteolytic degradation of the gelatin appeared as one weak band, and two clear bands (92, 72 and 67 kDa), were detected. EMD stimulatory effect on the expression of these bands was observed on d 4. On d 7, EMD stimulated the expression of 72 and 67 kDa bands, whereas EMD inhibited 92 kDa band expression. To confirm that this MMP activity was derived from the cells rather than from the EMD, the medium from a plate which had not been inoculated with cells was analyzed. Zymography of this sample did not produce any bands (data not shown), indicating that the MMP activity derived from the KUSA/A1 cells, not the EMD.

Northern blotting

In the culture condition for mRNA expression analysis, KUSA/A1 cells reached a confluence on d 4 and MN appeared on d 8 or 9. RNA was extracted from the culture on d 4, 7 and 10, and hybridized with various osteoblastic cDNA probes. The mRNA expression of COL I, OPN, BSP, TGF-β1 and OC is shown in Fig. 5. EMD enhanced mRNA expression of both COL I and OPN on d 4 and 7. However, the level of the enhancement was different at each time point. EMD did not affect BSP mRNA expression. The expression of TGF-β1 was not detected until d 7,

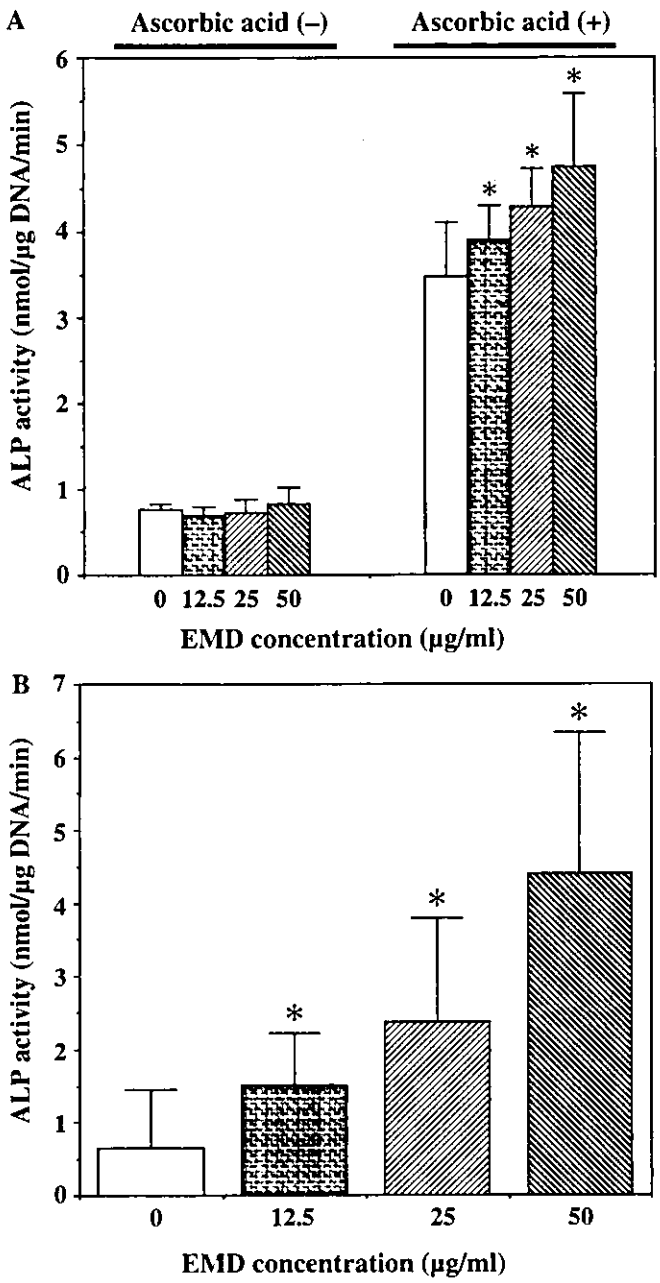

Fig. 2. Effect of EMD on ALP activity of ST2 cells (A) and KUSA/A1 cells (B). The cells were cultured in various concentrations of EMD; ALP activity of ST2 cells and KUSA/A1 cells was measured at d 16 and d 10, respectively. In ST2 cell culture, the medium with or without ascorbic acid was used. Data are presented as the mean + SD ($n = 4$). *Significantly different from the controls at $P < 0.05$.

and EMD enhanced TGF-β1 expression on d 7 and 10. The expression of OC was not detectable on d 4 or 7, and low expression of OC was observed on d 10. Extensive stimulation of OC expression by EMD treatment was observed on d 10.

EMD implantation

As shown in Fig. 6(A), the new bone formation in the bone defect appeared as radio-opaque areas in a soft X-ray photograph, and EMD stimulated new bone formation. The radio-opaque area of untreated-defect and defect treated with atelocollagen was approximately 10% and 35% of the original defect, respectively (Fig. 6B). In the group treated with atelocollagen and EMD, the radio-opaque area occupied 70% of the original bone defect (Fig. 6B). Histologically, newly formed mineralized bone and numerous migratory cells were evident in the pellets containing EMD (Fig. 6C). Two weeks after their implantation into the muscle, the pellets containing EMD had not induced mineralized tissue (data not shown).

Discussion

Commercially available EMD is a material extracted by acetic acid from porcine enamel matrix. The main component of EMD is amelogenin (3), although enamel matrix also contains other enamel proteins such as ameloblastin (known as amelin and sheathlin), and enamelin; it also contains several proteinases (31, 32). Since amelogenin is very hydrophobic and insoluble in water at neutral pH, EMD has similar solubility characteristics. In a clinical situation, immediately after EMD application, EMD probably forms aggregates on the denuded dentin surface. In the present study, EMD was precipitated after addition to the culture medium, after which the cells were inoculated. This method mimics the clinical situation and the same method has already been applied in other cell culture studies (13, 15).

PDL is a thin connective tissue between alveolar bone and cementum. Previous histological studies (33, 34) strongly suggest that PDL contains progenitor cells, specifically cementoblasts and osteoblasts. This concept is also supported by *in vitro* studies. In cell culture, PDL cells demonstrate osteoblastic characteristics such as high ALP activity (35, 36), cAMP production in response to parathyroid hormone and prostaglandin E_2 (36–38), and an ability to form MN (39, 40). A previous study has shown that EMD stimulates the proliferation, ALP activity, matrix production and MN formation of PDL cells (13), which correspond closely with the

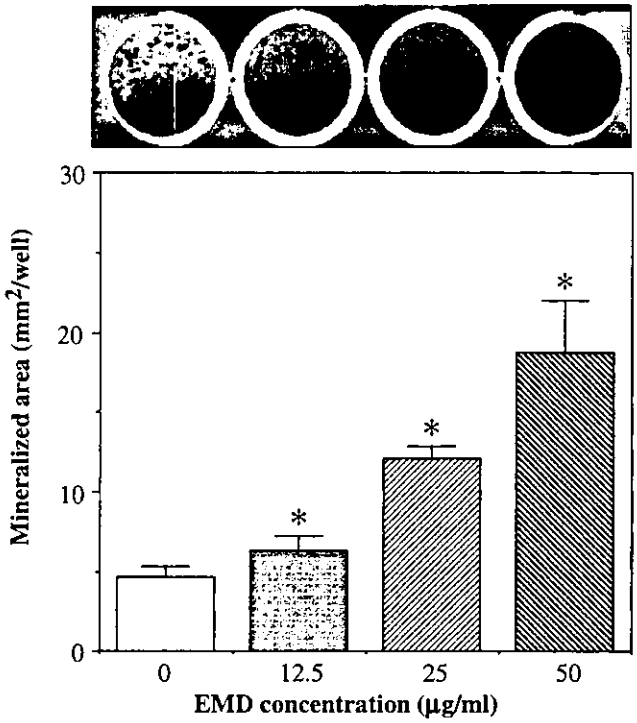

Fig. 3. Effect of EMD on MN formation of KUSA/A1 cells. KUSA/A1 cells were cultured in various concentrations of EMD. At d 10, the culture was fixed, stained with Alizarin Red S, and then mineralized area was measured. Stained image was presented in the upper panel. Data are presented as the mean + SD ($n = 6$). *Significantly different from the control at $P < 0.05$.

EMD stimulatory effect in periodontal tissue regeneration. Thus, EMD probably acts on cells of cementoblast or osteoblast lineage in PDL.

In the present study, we examined the effects of EMD on two different osteoblastic cells: ST2 cells and KUSA/A1 cells. ST2 cells are derived from mouse bone marrow and they differentiate to adipocytes or osteoblasts depending on culture conditions (18, 41). ST2 cells respond well to BMP-2, which subsequently induces high ALP activity (18). Supplementation with ascorbic acid leads ST2 cells to demonstrate high ALP activity (18). KUSA/A1 cells also originate from mouse bone marrow. They have the ability to form bone-like tissue when transplanted into mice, and also an ability to form MN in culture (19) and in the present study, KUSA/A1 cells could form MN very quickly and had high ALP activity immediately after the confluence. Therefore, compared to ST2 cells, KUSA/A1 cells are highly committed to osteoblastic linage and high osteoblastic activity.

In previous studies, the EMD effect on cellular proliferation has been shown to vary according to cell type. For example, EMD stimulates the proliferation of PDL cells and gingival fibroblasts (13, 15). However, EMD inhibits the proliferation of SCC25 cells (cells from human squamous cell carcinoma of the tongue) (17), whereas EMD does not affect the proliferation of other epithelial cells or HT1028 cells (13). The effect of EMD on cellular proliferation of several osteoblastic cells has been reported; this also suggests a diversity of cell responses to EMD (16, 42). In the present study, EMD stimulated KUSA/A1 cell proliferation although it did not affect ST2 cell proliferation which would confirm this. Thus, the effect of EMD on cellular proliferation depends on cell type.

Previous studies have shown that EMD effects on cellular ALP activity also depend on cell type. EMD stimulates the ALP activity of PDL cells, gingival fibroblasts (15), and some osteoblastic cells (normal human osteoblast-like cells and MG63 cells), whereas it does not stimulate ALP activity in 2T9 cells (16), an immature osteoprogenitor cell line. In the present study, when ST2 cells were induced by ascorbic acid to demonstrate osteoblastic differentiation and maturation, EMD stimulated the ALP activity of these ST2 cells. However, EMD did not affect the ALP activity of ST2 cells cultured without ascorbic acid supplementation. Furthermore, EMD stimulated the ALP activity of KUSA/A1 cells, which induced by supplementation of β-glycerophoshate. Thus, EMD could act on osteoblastic cells by increasing their ALP activity, but EMD could not induce initial production of ALP.

BMP-2 induces ALP activity in ST2 cells without ascorbic acid supplementation (18), whereas EMD did not induce ALP activity in ST2 cells without ascorbic acid supplementation. Intramuscular implantation of BMP-2 induces ectopic bone, whereas the pellets containing EMD did not induce ectopic bone formation in the present study. Boyan and her collaborators (20) have also reported that implantation of demineralized freeze-dried bone containing EMD in mouse muscle did not induce ectopic bone formation. Thus, the EMD does not have BMP-like osteoinductive activity.

EMD stimulated MN formation in KUSA/A1 cells. Although the mechanism and process of bone mineralization are not fully understood, it is thought that MN formation is the accumulated result of osteoblastic phenotype expression. In the present study, an increase in cell number was evident in the EMD-treated culture, which might partly contribute to the increase in MN. EMD stimulated the expression of osteoblastic phenotypes, including ALP activity and the production of some matrices. The stimulation of these phenotype expressions could significantly contribute to the increase in MN.

Matrix metalloproteinases (MMPs) are a family of related proteolytic enzymes that contain collagenases,

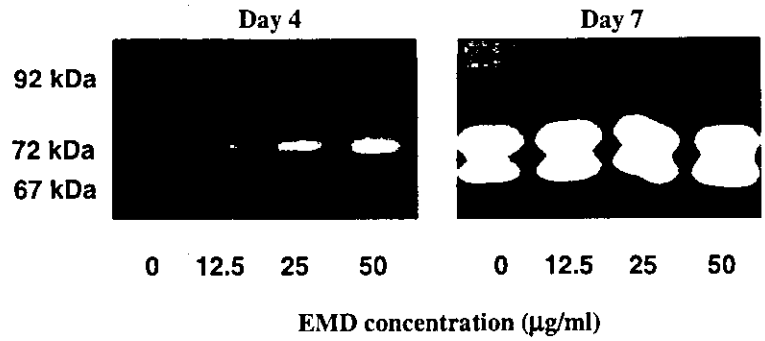

Fig. 4. Effect of EMD on MMP production in KUSA/A1 cells. KUSA/A1 cells were cultured in various concentrations of EMD. At d 4 and 7, medium was changed, conditioned medium was collected after 24 h, and then analyzed in gelatin zymography. The sample amount applied to the gels was corrected with the cell number of each sample. Thus, the intensity of the band means the relative MMP production of approximately same number of cells.

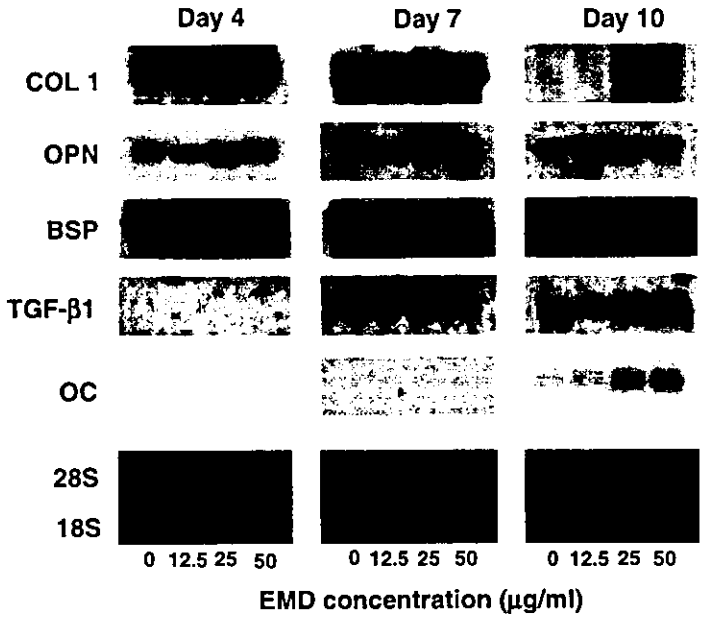

Fig. 5. Effect of EMD on mRNA expression of osteoblastic phenotypes in KUSA/A1 cells. mRNA expression of type I collagen (COL I), osteopontin (OPN), bone sialoprotein (BSP), transforming growth factor beta 1 (TGF-β1) and osteocalcin (OC) was analyzed in Northern blotting. The lowest panel represents the relative amount of the total RNA loaded in each lane.

gelatinases and stromelysins. The expression of MMPs as mediators of extracellular matrix remodeling appears critical to many growing or regenerating tissues (43–46). It is known that osteoblasts secrete MMP-1, 2, 3, 9, 10 and 13 (47–49), and these MMPs all have gelatinolytic activity with the exception of MMP-13. The present zymographic results showed three bands at 92, 72 and 67 kDa. Based on their molecular weight, they are probably attributable to a proenzyme form of MMP-9 and MMP-2, and an active form of MMP-2, respectively. MMP-2 and -9 are able to degrade native and denatured interstitial collagens as well as the basement membrane collagen (50). EMD stimulated MMP-2 production on d 4 and 7. In the EMD-treated culture of KUSA/A1 cells, a thick cell layer with matrix accumulation was evident. Thus, it is likely that EMD compensatively stimulates matrix production, although EMD also stimulates MMP production and matrix degradation. On d 7, the production of MMP-9 was inhibited by EMD. It has been reported that ALP-transfected osteosarcoma cells with high ALP activity inhibit the secretion of MMP-9 (51). The decrease in MMP-9 might correspond to the elevation of ALP in KUSA/A1 cells on d 7, although the physiological significance of this phenomenon is not clear.

It has been reported that EMD enhances extracellular matrix production, such as collagen and fibronectin, and TGF-β1 secretion in PDL cells (13–15). EMD also increases the level of TGF-β1 but has no effect on the production of collagen in the culture of osteoblastic MG63 cells (16). In KUSA/A1 cells, EMD strongly enhanced mRNA expression of COL I on d 4, TGF-β1 and OC on d 10. Although enhancement of MMP by EMD was detected by zymography, we speculate that the enhancement of the matrix proteins and TGF-β1 probably overcame the matrix degradation, resulting in matrix accumulation and the increase in MN formation.

Several *in vivo* experiments have demonstrated that EMD stimulates regeneration of the periodontal tissue including alveolar bone (5–7) and regeneration of bone defect in the femur (21). In these *in vivo* experiments, a variety of cells participate in bone regeneration. Thus, in the present study, we used calvarial bone defect model to clarify the direct effect of EMD on bone regeneration because the regeneration process of this bone defect model is probably simple. EMD stimulated new bone formation in a rat skull bone defect; however, EMD did not induce ectopic bone formation when it was intramuscularly implanted. Histologically, an increase in number of cells in the EMD pellets was evident. These cells in the pellets might have originated from the periosteum and endosteum of the bony rim of the defect. Since EMD enhances the

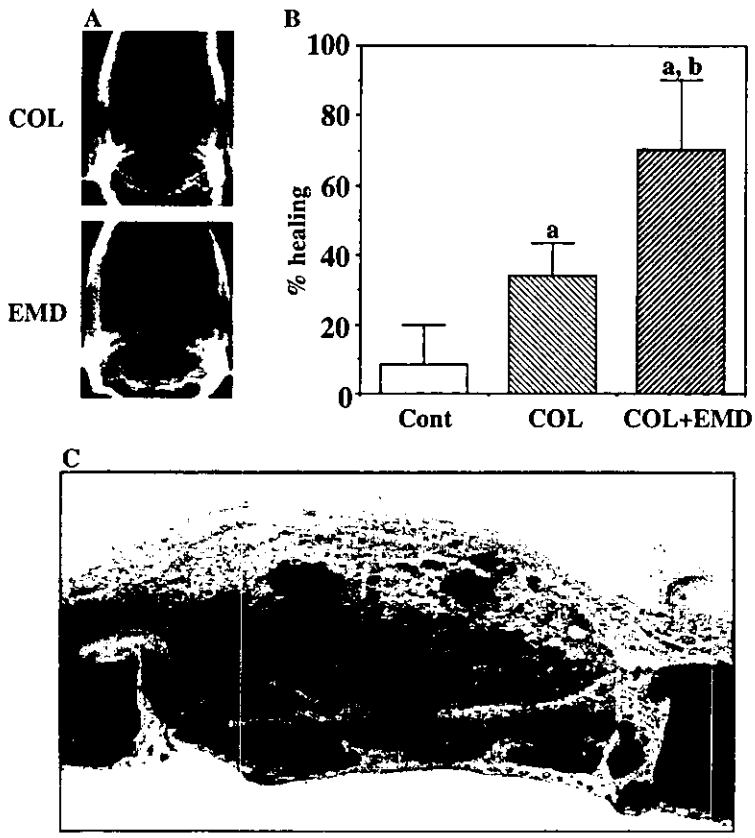

Fig. 6. Effect of EMD on healing of rat skull defect. (A) Soft X-ray photographs were taken at 2 weeks after the operation. Right defects were filled with atelocollagen (upper; COL) or with atelocollagen containing EMD (lower; COL + EMD). Left side (upper and lower) was control (filled with nothing). (B) Healing of the skull defects after various treatments. Radiopacity area of defects was measured and calculated the percentage of their occupied area of the defect. Data are presented as the mean + SD ($n = 4$: each experimental groups. $n = 8$: control group). Significantly different from the control or COL group at $^{a}P < 0.05$, $^{b}P < 0.05$, respectively. (C) Histological section of EMD treated group. At 2 weeks after the operation, new formed bone and mineralized deposit were observed in implantation of EMD (toluidine blue staining).

migration of PDL cells in the *in vitro* wound healing model (14), a similar phenomenon could have occurred at the healing site of the skull bone defect treated with EMD.

Veis *et al.* (52) have reported that short forms of the spliced products of rat amelogenin induce chondrogenic phenotypes in cultures of embryonic rat muscle cells, and that implantation of these recombinant amelogenins in muscle induces the formation of ectopic mineralized tissue. However, in the present study, EMD pellets did not induce such ectopic mineralization. It is certain that EMD contains various types of amelogenins; however, it is unlikely that EMD contains similar molecules of inducing ectopic mineralization. Boyan and her collaborators (20) have reported that EMD stimulates the bone formation ectopically induced by BMP although EMD does not have BMP-like osteoinductive activity. Their findings and our *in vivo* results indicate that EMD has an ability to stimulate the bone formation that is induced by BMP or during the bone regeneration process.

In conclusion, although the effects of EMD on osteoblastic cells are complex, the overall effect of EMD on osteoblastic cells is stimulatory rather than inhibitory, which could contribute favorably to bone regeneration. EMD itself is not an osteoinductive material like BMPs; however, it may have potential therapeutic as a material for bone regeneration.

Acknowledgements

This study was supported by a Grant-in Aid from the Japanese Ministry of Education, Culture, Sports, Science and Technology (11470460) and the Japan Society for the Promotion of Science (96I00205).

References

1. Slavkin HC. Towards a cellular and molecular understanding of periodontics: Cementogenesis revisited. *J Periodontol* 1976;**47**:249–255.
2. Hammarström L. Enamel matrix, cementum development and regeneration. *J Clin Periodontol* 1997;**24**:658–668.
3. Hammarström L, Heijl L, Gestrelius S. Periodontal regeneration in a buccal dehiscence model in monkeys after application of enamel matrix proteins. *J Clin Periodontol* 1997;**24**:669–677.
4. Heijl L. Periodontal regeneration with enamel matrix derivative in one human experimental defect. A case report. *J Clin Periodontol* 1997;**24**:693–696.
5. Araujo MG, Lindhe J. GTR treatment of degree III furcation defects following application of enamel matrix proteins. An experimental study in dogs. *J Clin Periodontol* 1998;**25**:524–530.
6. Sculean A, Donos N, Brecx M, Reich E, Karring T. Treatment of intrabony defects with guided tissue regeneration and enamel-matrix-proteins – An experimental study in monkeys. *J Clin Periodontol* 2000;**27**:466–472.
7. Sculean A, Donos N, Reich E, Karring T, Brecx M. Regeneration of oxytalan fibres in different types of periodontal defects: a histological study in monkeys. *J Periodont Res* 1998;**33**:453–459.
8. Heden G, Wennstrom J, Lindhe J. Periodontal tissue alterations following Emdogain treatment of periodontal sites with angular bone defects. A series of case reports. *J Clin Periodontol* 1999;**26**:855–860.
9. Heijl L, Heden G, Svardstrom G, Ostgren A. Enamel matrix derivative (EMDOGAIN) in the treatment of intrabony periodontal defects. *J Clin Periodontol* 1997;**24**:705–714.
10. Rasperini G, Ricci G. Surgical technique for treatment of infrabony defects with enamel matrix derivative (Emdogain): 3 case reports. *Int J Periodontics Restorative Dent* 1999;**19**:578–587.

11. Sculean A, Reich E, Chiantella GC, Brecx M. Treatment of intrabony periodontal defects with an enamel matrix protein derivative (Emdogain). a report of 32 cases. *Int J Periodontics Restorative Dent* 1999;**19**:157–163.
12. Sculean A, Donos N, Karring T *et al.* Healing of human intrabony defects following treatment with enamel matrix proteins or guided tissue regeneration. *J Periodont Res* 1999;**34**:310–322.
13. Gestrelius S, Andersson C, Lidstrom D, Hammarström L, Somerman M. *In vitro* studies on periodontal ligament cells and enamel matrix derivative. *J Clin Periodontol* 1997;**24**:685–692.
14. Hoang AM, Oates TW, Cochran DL. *In vitro* wound healing responses to enamel matrix derivative. *J Periodontol* 2000;**71**:1270–1277.
15. Van der Pauw MT, Van den Bos T, Everts V, Beertsen W. Enamel matrix-derived protein stimulates attachment of periodontal ligament fibroblasts and enhances alkaline phosphatase activity and transforming growth factor beta 1 release of periodontal ligament and gingival fibroblasts. *J Periodontol* 2000;**71**:31–43.
16. Schwartz Z, Carnes DL Jr, Boyan BD *et al.* Porcine fetal enamel matrix derivative stimulates proliferation but not differentiation of pre-osteoblastic 2T9 cells, inhibits proliferation and stimulates differentiation of osteoblast-like MG63 cells, and increases proliferation and differentiation of normal human osteoblast NHOst cells. *J Periodontol* 2000;**71**:1287–1296.
17. Kawase T, Okuda K, Yoshie H, Burns DM. Cytostatic action of enamel matrix derivative (EMDOGAIN®) on human oral squamous cell carcinoma-derived SCC25 epithelial cells. *J Periodont Res* 2000;**35**:291–300.
18. Otsuka E, Yamaguchi A, Hirose S, Hagiwara H. Characterization of osteoblastic differentiation of stromal cell line ST2 that is induced by ascorbic acid. *Am J Physiol* 1999;**277**:C132–C138.
19. Umezawa A, Maruyama T, Segawa K, Shadduck RK, Waheed A, Hata J. Multipotent marrow stromal cell line is able to induce hematopoiesis *in vivo*. *J Cell Physiol* 1992;**151**:197–205.
20. Boyan BD, Weesner TC, Schwartz Z *et al.* Porcine fetal enamel matrix derivative enhances bone formation induced by demineralized freeze dried bone allograft *in vivo*. *J Periodontol* 2000;**71**:1278–1286;.
21. Kawana F, Sawae Y, Sasaki T *et al.* Porcine enamel matrix derivative enhances trabecular bone regeneration during wound healing of injured rat femur. *Anat Rec* 2001;**264**:438–446.
22. Labarca C, Paigen K. A simple, rapid, and sensitive DNA assay procedure. *Anal Biochem* 1980;**102**:344–352.
23. Porstmann T, Ternynck T, Avrameas S. Quantitation of 5-bromo-2-deoxyuridine incorporation into DNA: an enzyme immunoassay for the assessment of the lymphoid cell proliferative response. *J Immunol Meth* 1985;**82**:169–179.
24. Bessey OA, Lowry OH, Breck MJ. A method for the rapid determination of alkaline phosphatase with five cubic millimeters of serum. *J Biol Chem* 1946;**164**:312–326.
25. Chomczynski P, Sacchi N. Single-step method of RNA isolation by acid guanidinium thiocyanate-phenol-chloroform extraction. *Anal Biochem* 1987;**162**:156–159.
26. Genovese C, Rowe D, Kream B. Construction of DNA sequences complementary to rat alpha 1 and alpha collagen mRNA and their use in studying the regulation of type I collagen synthesis by 1,25-dihydroxyvitamin D. *Biochemistry* 1984;**23**:6210–6216.
27. Nomura S, Wills AJ, Edwards DR, Heath JK, Hogan BL. Developmental expression of 2ar (osteopontin) and SPARC (osteonectin) as revealed by in situ hybridization. *J Cell Biol* 1988;**106**:441–450.
28. Chen JK, Shapiro HS, Wrana JL, Reimers S, Heersche JN, Sodek J. Localization of bone sialoprotein (BSP) expression to sites of mineralized tissue formation in fetal rat tissues by in situ hybridization. *Matrix* 1991;**11**:133–143.
29. Celeste AJ, Rosen V, Buecker JL, Kriz R, Wang EA, Wozney JM. Isolation of the human gene for bone gla protein utilizing mouse and rat cDNA clones. *EMBO J* 1986;**5**:1885–1890.
30. Derynck R, Jarrett JA, Chen EY, Goeddel DV. The murine transforming growth factor-beta precursor. *J Biol Chem* 1986;**261**:4377–4379.
31. Fincham AG, Hu Y, Lau EC, Slavkin HC, Snead ML. Amelogenin post-secretory processing during biomineralization in the postnatal mouse molar tooth. *Arch Oral Biol* 1991;**36**:305–317.
32. Termine JD, Belcourt AB, Christner PJ, Conn KM, Nylen MU. Properties of dissociatively extracted fetal tooth matrix proteins. I. Principal molecular species in developing bovine enamel. *J Biol Chem* 1980;**255**:9760–9768.
33. Buser D, Warrer K, Karring T. Formation of a periodontal ligament around titanium implants. *J Periodontol* 1990;**61**:597–601.
34. Herr Y, Matsuura M, Lin WL, Genco RJ, Cho MI. The origin of fibroblasts and their role in the early stages of horizontal furcation defect healing in the beagle dog. [published erratum appears in *J Periodontol* 66: 915–923; 1995.] *J Periodontol* 1995;**66**:716–730.
35. Nojima N, Kobayashi M, Shionome M, Takahashi N, Suda T, Hasegawa K. Fibroblastic cells derived from bovine periodontal ligaments have the phenotypes of osteoblasts. *J Periodont Res* 1990;**25**:179–185.
36. Piche JE, Carnes DL Jr, Graves DT. Initial characterization of cells derived from human periodontia. *J Dent Res* 1989;**68**:761–767.
37. Nohutcu RM, McCauley LK, Horton JE, Capen CC, Rosol TJ. Effects of hormones and cytokines on stimulation of adenylate cyclase intracellular calcium concentration in human and canine periodontal-ligament fibroblasts. *Arch Oral Biol* 1993;**38**:871–879.
38. Rao LG, Moe HK, Heersche JN. *In-vitro* culture of porcine periodontal ligament cells: response of fibroblast-like and epithelial-like cells to prostaglandin E1, parathyroid hormone and calcitonin and separation of a pure population fibroblast-like cells. *Arch Oral Biol* 1978;**23**:957–964.
39. Groeneveld MC, Everts V, Beertsen W. Formation of afibrillar acellular cementum-like layers induced by alkaline phosphatase activity from periodontal ligament explants maintained *in vitro*. *J Dent Res* 1994;**73**:1588–1592.
40. Ramakrishnan PR, Lin WL, Sodek J, Cho MI. Synthesis of noncollagenous extracellular matrix proteins during development of mineralized nodules by rat periodontal ligament cells *in vitro*. *Calcif Tissue Int* 1995;**57**:52–59.
41. Yamaguchi A, Ishizuya T, Yoshiki S *et al.* Effects of BMP-2, BMP-4, and BMP-6 on osteoblastic differentiation of bone marrow-derived stromal cell lines, ST2 and MC3T3-G2/PA6. *Biochem Biophys Res Commun* 1996;**220**:366–371.
42. Tokiyasu Y, Takata T, Saygin E, Somerman M. Enamel factors regulate expression of genes associated with cementoblasts. *J eriodontol* 2000;**71**:1829–1839.
43. Chin JR, Werb Z. Matrix metalloproteinases regulate morphogenesis, migration and remodeling of epithelium, tongue skeletal muscle and cartilage in the mandibular arch. *Development* 1997;**124**:1519–1530.
44. Johansson N, Saarialho-Kere U, Kahari VM *et al.* Collagenase-3 (MMP-13) is expressed by hypertrophic chondrocytes, periosteal cells, and osteoblasts during human fetal bone development. *Dev Dyn* 1997;**208**:387–397.
45. La Fleur M, Underwood JL, Rappolee DA, Werb Z. Basement membrane and repair of injury to peripheral nerve: defining a potential role for macrophages, matrix metalloproteinases, and tissue inhibitor of metalloproteinases-1. *J Exp Med* 1996;**184**:2311–2326.
46. Yang EV, Bryant SV. Developmental regulation of a matrix metalloproteinase during regeneration of axolotl appendages. *Dev Biol* 1994;**166**:696–703.

47. Bord S, Horner A, Beeton CA, Hembry RM, Compston JE. Tissue inhibitor of matrix metalloproteinase-1 (TIMP-1) distribution in normal and pathological human bone. *Bone* 1999;**24:** 229–235.
48. Breckon JJ, Papaioannou S, Meikle MC *et al.* Stromelysin (MMP-3) synthesis is up-regulated in estrogen-deficient mouse osteoblasts *in vivo* and *in vitro*. *J Bone Miner Res* 1999;**14:**1880–1890.
49. Panagakos FS, Kumar S. Modulation of proteases and their inhibitors in immortal human osteoblast-like cells by tumor necrosis factor-alpha *in vitro*. *Inflammation* 1994;**18:**243–265.
50. Lorenzo JA, Pilbeam CC, Kalinowski JF, Hibbs MS. Production of both 92- and 72-kDa gelatinases by bone cells. *Matrix* 1992;**12:**282–290.
51. Manara MC, Baldini N, Scotlandi K *et al.* Mar Reversal of malignant phenotype in human osteosarcoma cells transduced with the alkaline phosphatase gene. *Bone* 2000;**26:**215–220.
52. Veis A, Tompkins K, Healy KE *et al.* Specific amelogenin gene splice products have signaling effects on cells in culture and in implants *in vivo*. *J Biol Chem* 2000;**275:**41263–41272.

Oncogene (2003) 22, 1–9

www.nature.com/onc

ORIGINAL PAPERS

Upregulation of Id2, an oncogenic helix-loop-helix protein, is mediated by the chimeric EWS/ets protein in Ewing sarcoma

Mariko Fukuma[1], Hajime Okita[1], Jun-ichi Hata[1] and Akihiro Umezawa[1,*]

Department of Pathology, Keio University School of Medicine, 35 Shinanomachi, Shinjuku-ku, Tokyo 160-8582, Japan

The chromosomal translocation specifically linked to the Ewing sarcoma family results in the generation of fusion proteins comprising the amino terminal portion of EWS and the DNA-binding domain of ets transcription factors. The EWS/ets chimeric proteins act as aberrant transcription factors leading to tumorigenic processes. We searched for genes specifically activated in Ewing sarcoma cells but not in other tumor cell lines using the gene array technique, and found significantly enhanced expression of the Id2 gene. High levels of Id2 transcripts were detected in Ewing sarcoma cell lines and tumor tissues. The EWS/ets chimeric proteins activated the Id2 gene via the 5′-upstream promoter sequence. Chromatin-immunoprecipitation revealed a direct interaction of EWS/Fli-1 with the promoter regions of the Id2, TGF-β type II receptor, cyclin D1, and c-myc genes. Since EWS/Fli-1 transactivates c-myc, a cooperative action of the chimeric protein and c-myc leads to overexpression of Id2. In the present study, we suggest that Id2 is a target of the chimeric proteins and that the c-myc/Id2 pathway plays a pivotal role in the tumorigenic processes provoked by EWS/ets proteins.
Oncogene (2003) **22**, 1–9. doi:10.1038/sj.onc.1206055

Keywords: Ewing sarcoma; Id2; EWS/ets; chimeric protein

Introduction

Ewing sarcoma and peripheral primitive neuroectodermal tumor (PNET) are referred to as the Ewing sarcoma family of tumors that encompasses a group of biologically identical small round cell tumors. Ewing sarcoma is the second most common solid tumor found in the bone and soft tissue of children and young adults. Despite advances in multimodal cancer therapy, the overall long-term survival rate is still less than 60% (Paulussen *et al.*, 2001). Owing to the lack of unequivocal lineage markers, the histogenesis of Ewing sarcoma remains controversial. A specific chromosomal translocation, t(11;22)(q24:q12), has been reported in more than 80% of Ewing sarcomas. This chromosomal translocation results in the fusion of the 5′ segment of the EWS gene on chromosome 22 with the 3′ segment of the Fli-1 gene on chromosome 11 (Delattre *et al.*, 1992). The EWS gene also fuses with other members of the ets family, for example, ERG (Sorensen *et al.*, 1994), ETV1 (Jeon *et al.*, 1995), FEV (Peter *et al.*, 1997), and E1AF, which we have reported previously (Urano *et al.*, 1996, 1998).

Ets oncoproteins contain an 85 amino acid long domain, called the ets-domain, which has been conserved among members of the ets family. With this domain they bind as monomers to core 5′-GGA(A/T)-3′ sequences, and the flanking sequences of this core determine the affinity and specificity of ets proteins to these target sequences. The functional synergy between ets oncoproteins with other transcription factors such as AP-1, Sp-1, and c-myb has been reported (Wasylyk *et al.*, 1990; Gegonne *et al.*, 1993; Nelsen *et al.*, 1993; Pankov *et al.*, 1994). Ets family members are involved in the developmental processes of various lineages such as T cell, B cell, and neural cells. The EWS/ets chimeric proteins work as aberrant transcription factors that interfere with this legitimate development and lead to oncogenesis of Ewing sarcomas.

The target genes of EWS/ets oncoproteins have extensively been investigated to understand the tumorigenic mechanism in Ewing sarcoma. EWS/Fli-1 is a strong transactivator of the c-myc promoter (Bailly *et al.*, 1994). Several genes such as EAT-2 (Thompson *et al.*, 1996), stromelysin (Braun *et al.*, 1995), and fringe (May *et al.*, 1997) are reported to be upregulated, while TGF-β type II receptor (TGFβIIR) (Im *et al.*, 2000), p21 (Matsumoto *et al.*, 2001), and p57KIP2 (Dauphinot *et al.*, 2001) are downregulated. Furthermore, EWS/Fli-1 interacts with hsRPB7, a subunit of human RNA polymerase II (Petermann *et al.*, 1998), and the EWS/Fli-1 fusion protein alters the IGF-IR signaling pathway (Toretsky *et al.*, 1997).

Since the ets proteins augment expression of various types of transcription factors, we presumed that there would be other genes whose expression is modified by the occurrence of the chimeric proteins. We sought for genes specifically expressed in Ewing sarcoma and found enhanced expression of the Id2 gene. Id proteins are helix-loop-helix (HLH) proteins lacking the basic amino acid domain necessary to bind DNA. Id proteins

*Correspondence: A Umezawa, Department of Pathology, Keio University, School of Medicine, 35 Shinanomachi, Shinjuku-ku, Tokyo 160-8582, Japan; E-mail: umezawa@1985.jukuin.keio.ac.jp
Received 9 April 2002; revised 17 September 2002; accepted 19 September 2002

function in a dominant negative manner by sequestering ubiquitously expressed (eg, E12, E47, and E2-2) or cell-type restricted (eg, Tal-1 and MyoD) basic HLH transcription factors, thereby blocking the binding of dimerized basic HLH proteins to DNA. They regulate transcription factors that are involved in developmental processes such as myogenesis, neurogenesis, bone morphogenesis, lymphopoiesis hematopoiesis, and myeloid differentiation (Norton *et al.*, 1998). In transgenic chicken embryos, the ectopic expression of Id2 converts ectodermal cells to a neural crest fate (Martinsen and Bronner-Fraser, 1998). Id2−/− mice lack lymph nodes and Peyer's patches, and show a reduced population of natural killer cells (Yokota *et al.*, 1999). Id proteins are also involved in cellular proliferation processes. The growth-suppressive activity of retinoblastoma proteins (RB) is reversed by Id2 through physical interactions between those proteins (Iavarone *et al.*, 1994). High levels of Id2 reverse the growth suppressive activity of cyclin-dependent kinase inhibitors, p16 and p21 (Lasorella *et al.*, 1996). Furthermore, the oncoproteins of the myc family require Id2 to bypass the regulatory function of RB (Lasorella *et al.*, 2000). Thus, Id2, a protein required to maintain the timing of differentiation in mammalian development, is also a potent effector in the tumorigenic process of human cancer. Here we demonstrate extremely high levels of Id2 expression in Ewing sarcomas, presumably caused by the direct interaction between EWS/ets chimeric proteins and the promoter region of the Id2 gene.

Results

Gene expression analysis with the human cDNA array

We employed a cDNA expression array system to search for candidate target genes of EWS/ets chimeric proteins. Gene expression profiles of NCR-EW2 with the EWS/Fli-1, W-ES with the EWS/ERG, and NCR-EW3 with the EWS/E1AF, and NCR-G3 embryonal carcinoma are shown in Figure 1. Significantly high levels of c-myc and cyclin D transcripts were detected in all the cells tested. However, the levels were somewhat lower in NCR-G3 than in Ewing sarcoma cells. The highest level of Id2 transcripts was detected in Ewing sarcoma cells (Figure 1a–c), while it was below detectable level in NCR-G3 (Figure 1d). As Id2 regulates cellular differentiation into various lineages, the extraordinarily high level of Id2 expression may play a crucial role in the tumorigenesis of Ewing sarcoma. Similar levels of high expression were also seen in 40S ribosomal protein S-19, heat-shock 27 kD protein 1, glutathione S-transferase P, DNA-binding protein TAX and TAXREB67, RNA polymerase elongation factor SIII, guanine nucleotide-binding protein G-S, Y-box binding protein-1, proliferation-associated protein PAG, and thymosin beta-10 in all four cell lines. Why these transcripts increased still remains unclear.

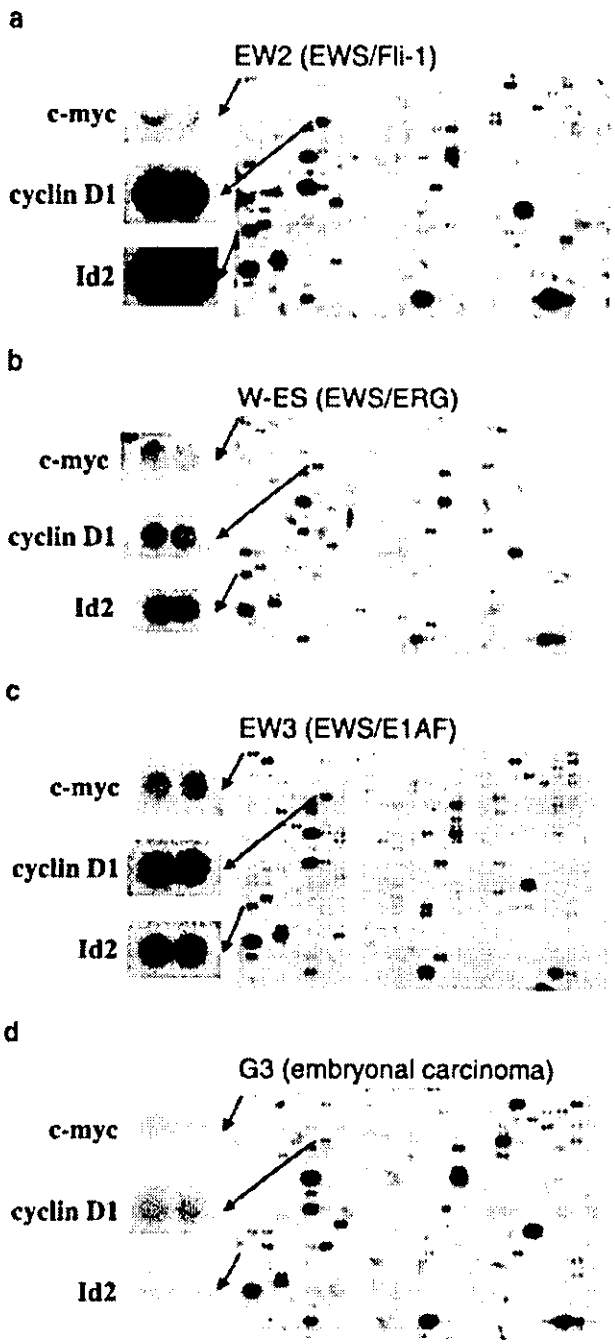

Figure 1 Gene expression profiles in Ewing sarcoma and embryonal carcinoma cells. ^{32}P-labeled cDNA probes were generated from each polyA$^+$ RNA sample isolated from the cells, NCR-EW2 with EWS-Fli-1 (**a**), W-ES with EWS/ERG (**b**), NCR-EW3 with EWS/E1AF (**c**), and NCR-G3 embryonal carcinoma (**d**). The spots of c-myc, cyclin D1 and Id2 are enlarged and shown on the left

Id2 expression in Ewing sarcoma

The enhanced expression of the Id2 gene was also detected by Northern blot analysis. Id2 was highly expressed in all the Ewing sarcoma cell lines, as well as in neuroblastoma cells, but was below a detectable level in NCR-G3 (Figure 2) and in HeLa cells (data not

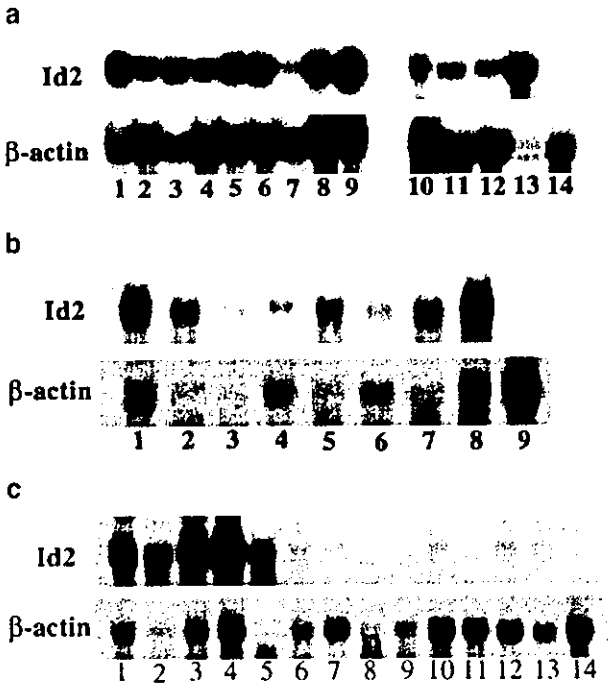

Figure 2 Northern blot analysis of Id2 expression. (a): Id2 transcripts in cell lines from Ewing sarcoma and other tumors. Lane 1: NCR-EW2 with EWS/Fli-1; Lane 2: NCR-EW3 with EWS/EIAF; Lanes 3 and 13: W-ES with EWS/ERG; Lane 4: SYM-1 with EWS/Fli-1; Lane 5: RD-ES with EWS/Fli-1; Lane 6: SCCH196 with EWS/Fli-1; Lane 7: EES-1 with EWS/Fli-1; Lane 8: EW93 with EWS/Fli-1; Lane 9: KU-9 with EWS/Fli-1; Lane 10: KNB-1 neuroblastoma; Lane 11: PN-1 (known chimera gene could not be detected); Lane 12: MURAOKA with EWS/Fli-1; Lane 14: NCR-G3 embryonal carcinoma. (b): Id2 transcripts in Ewing sarcoma tissue (Lanes 2–8: cases 1–7 in Table 2). Lane 1: NCR-EW2, Lane 9: NCR-G3. (c): Comparison of Id2 expression levels in tumor tissues. Lanes 2–5: cases 8,9,7 and 10 of Ewing sarcoma; Lanes 6–9: cases 11–14 of rhabdomyosarcoma; Lanes 10–14: cases 15–18 of neuroblastoma in Table 2. Lane 1: NCR-EW2 as a positive control

shown). Total RNA was also extracted from frozen blocks of tissues that had been diagnosed as Ewing sarcoma by immunohistochemistry and the detection of chimeric genes. Id2 was detected in all tissue samples from Ewing sarcoma. We further examined the expression of Id2 in comparison with other undifferentiated solid tumors in children, rhabdomyosarcoma, and neuroblastoma. Tumors are randomly selected from freeze-stock specimens. The chimeric genes in Ewing sarcoma specimens were found to be EWS/Fli-1. Significantly higher levels of Id2 transcripts were detected in Ewing sarcoma than in rhabdomyosarcoma and neuroblastoma. The high level of Id2 in Ewing sarcoma leads us to speculate that the EWS/ets gene products directly promote Id2 expression *in vivo*.

Activation of the Id2 promoter by the EWS/ets chimeric protein

We examined whether EWS/ets proteins activate the promoter of the Id2 gene. A DNA segment containing the *cis*-regulatory element of Id2, nucleotide −221 to −46, was placed in either the forward (IdL-FWD) or reverse (IdL-REV) direction upstream of the luciferase gene. The reporter gene was co-transfected with an EWS/ets expression vector and phRL-TK reference vector. The luciferase activity was significantly enhanced with EWS/Fli-1, EWS/ERG, and EWS/EIAF (Figure 3a–e). The reversely ligated promoter produced almost the same results. This result is consistent with the fact that the upstream regulatory element usually works in either direction in the transcription process. Next, we introduced point mutations into the ets consensus sequence to analyze whether this sequence is required for the promoter activity (Figure 3d). The promoter region contains a canonical ets consensus sequence 50-bp downstream of the E-box where basic-HLH transcription factors interact. When the guanine (−156) was replaced with thymine the enhancing effect of EWS/Fli-1 decreased by about 25% (Figure 3e). Similar results were obtained when the adenine (−155) was replaced with cytosine. Thus, the ets consensus sequence is required to exert increased activation. When the adenine (−204) in the E-box was replaced with thymine, or thymine (−201) was replaced with cytosine, the promoter activity was significantly reduced by 80%. Similar results were obtained when EWS/EIAF was co-transfected as an effector (Figure 3f). Promoter activity was reduced by 30% after ets point mutation and by 70% after E-box mutation. A reporter construct IdS, lacking the E-box and juxtaposed sequences, was produced to allow analysis of the activation effect of chimeric proteins in the absence of E-box influence. Single nucleotide mutations in the ets site of the truncated promoter, at nucleotide positions −156 and −155, decreased the promoter activity by 46 and 45%, respectively (Figure 3g). These results imply that these two promoter elements, the E-box and the ets recognition sequence, contribute independently in the activation of the regulatory element of the Id2 gene.

The reporter genes were transfected into Ewing sarcoma cell lines to investigate whether they are functional in cells with native chimeric genes. In the NCR-EW2 cell line with EWS/Fli-1, both IdL and IdS were active (Figure 4a). The mutations at the ets site resulted in a decrease in activity by 30–40%. Similarly, in W-ES cells with EWS/ERG, the ets mutations diminished the promoter activity by 50–60% (Figure 4b). Owing to very low transfection efficiency no transcriptional activity was detected in NCR-EW3 cells with EWS/EIAF.

Binding of EWS/ets protein to the Id2 cis-regulatory element in vivo

We then used the chromatin immunoprecipitation (ChIP) technique to examine whether EWS/ets gene products interact with the Id2 promoter region. Chromatin was extracted from formaldehyde-treated cells, and anti-Fli-1 antibody or a corresponding amount of nonimmune IgG was added. Analysis by PCR detected

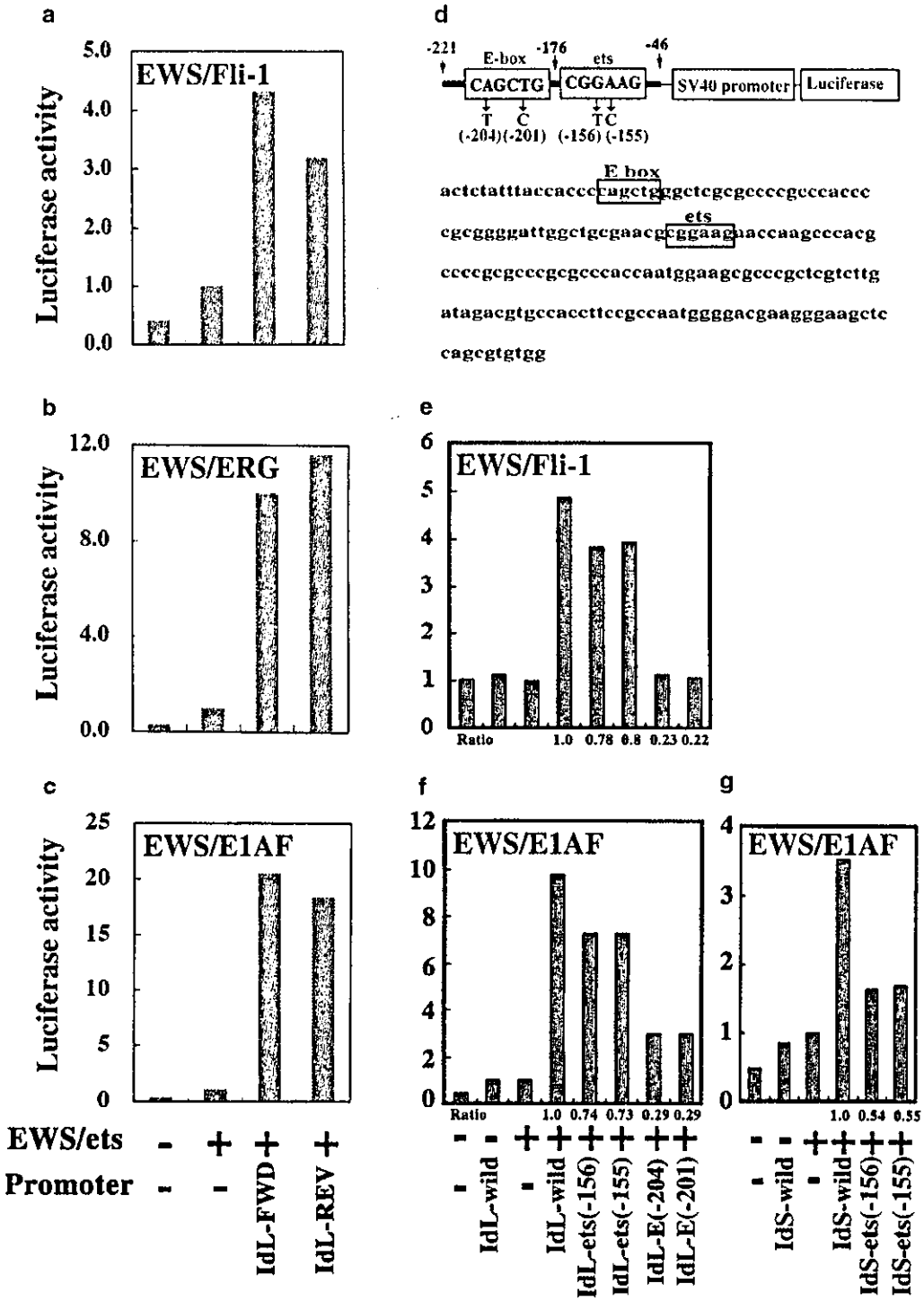

Figure 3 Transactivation of the Id2 promoter by the EWS/ets chimeric genes. HeLa cells were cotransfected with either Id2 promoter-luciferase reporter (IdL-FWD: forward, IdL-REV: reverse) or an empty reporter (pGL3-promoter vector), and an EWS/Fli-1 (**a**), EWS/ERG (**b**) or EWS/E1AF (**c**) expression vector. Furthermore, the phRL-TK vector was cotransfected to normalize the transfection efficiency. The luminescence intensity is expressed as a ratio of reporter vector to the phRL-TK reference vector. (**d**) The upstream regulatory region of the Id2 gene and the mutation map of the luciferase reporter gene. EWS/Fli-1 (**e**) or EWS/E1AF (**f**) was transfected as a transactivator of the mutant Id2 promoter. A comparison of the luciferase ratio of the mutated constructs and the wild-type promoter is shown at the foot of each column, and the wild type is regarded as 1.0 (**e–g**). (**g**) Reporter genes under the regulation of the truncated promoter sequence, −176 to −46, were cotransfected with EWS/E1AF into HeLa cells. Experiments were repeated at least three times and typical results are shown here

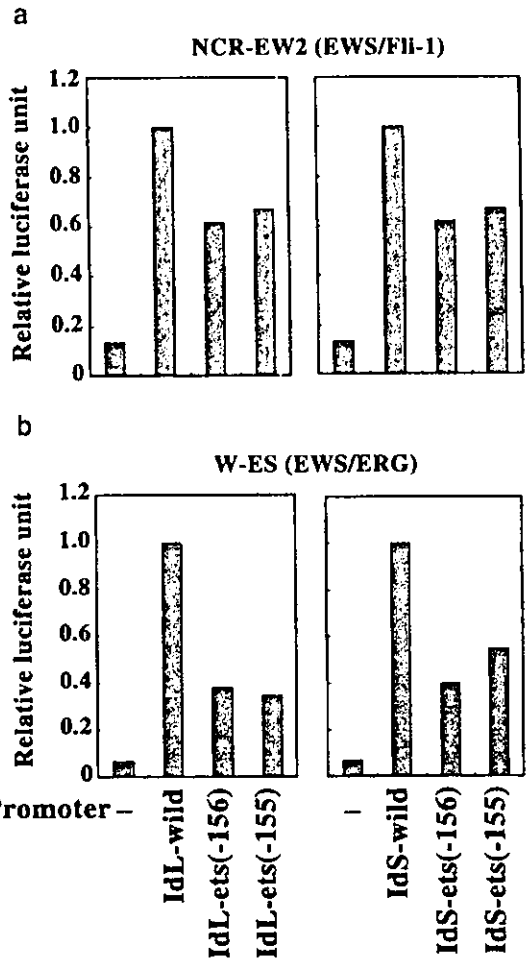

Figure 4 *cis*-transactivation of the Id2 promoter in Ewing sarcoma cells. Reporter genes were transfected into NCR-EW2 cells with EWS Fli-1 (a) and into W-ES cells with EWS/ERG (b). The luminescence intensity is expressed as a ratio of reporter vector to the phRL-TK reference vector, and the wild type (IdL-wild or IdS-wild) is regarded as 1.0 Experiments were repeated twice and each experiment was performed on duplicate wells

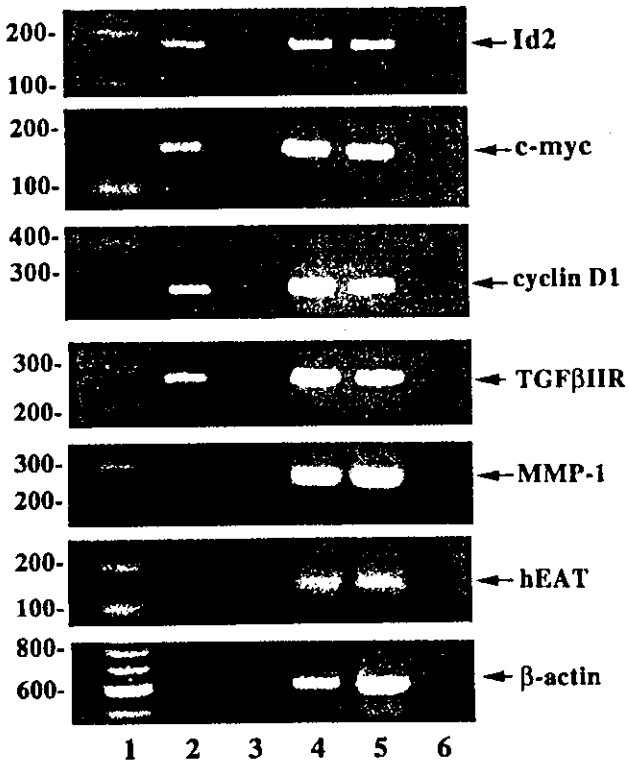

Figure 5 Binding of EWS Fli-1 to the Id2 promoter *in vivo*. Crosslinked chromatin was prepared from NCR-EW2 cells. Chromatin was incubated with anti-Fli-1 antibody or normal rabbit IgG, and the regulatory fragments were amplified by PCR from the immunoprecipitates. The DNA templates are as follows: Lane 2, immunoprecipitates with anti-Fli-1; Lane 3, immunoprecipitates with normal rabbit IgG; Lane 4, chromatin DNA corresponding to 0.05% of total input DNA; Lane 5, chromatin DNA from human placenta; Lane 6, distilled H_2O as a negative control; Lane 1, molecular size markers. Molecular sizes are represented as base pair on the left of the panels

specific promoter regions of the Id2, *c*-myc, cyclin D1 and TGFβIIR genes in immunoprecipitates with anti-Fli-1 antibody but not with the nonimmune IgG (Figure 5). Neither the *cis*-element containing ets consensus sequences of EAT/MCL-1 nor of the matrix metalloproteinase-1 (MMP-1) was detected in either of the immunoprecipitates. Furthermore, the β-actin fragment was also undetected in either immunoprecipitate. These results indicate that the binding of the chimeric protein to the Id2 promoter region is specific. It is unlikely that the PCR products are from an intact Fli-1-chromatin complex, because Fli-1 transcripts are not detected in Ewing sarcoma cells (Bailly *et al*., 1994), and a single band identical to the EWS/Fli-1 protein was detected in the immunoprecipitates from Ewing cells by the anti-Fli-1 antibody. We here demonstrate that the EWS/Fli-1 gene products interact directly with the regulatory elements of Id2, c-myc, cyclin D and TGFβIIR.

Discussion

In this study, we have demonstrated a direct transactivation of Id2 by EWS/ets chimeric proteins. Extremely high levels of Id2 gene expression were specifically observed in Ewing sarcoma cells and tumor tissues but not in embryonal carcinoma cells, rhabdomyosarcoma or neuroblastoma. We have also presented evidence suggesting that the EWS/ets proteins activate the Id2 gene through the direct interaction between the Id2 promoter and EWS/Fli-1 *in vivo*.

The substantial increase of Id2 by the EWS/ets chimeric proteins seemed to be functionally mediated through ets recognition sequences and E-box. Three E-box/ets clusters and several other ets-like sequences exist in the 2-kb enhancing region of the Id2 gene. The E-box located 50-bp upstream of the ets consensus sequence is important for the Id2 promoter activity. The decrease in Id2 promoter activity caused by point mutations in the E-box suggests that E-box-binding proteins, predominantly c-myc, and ets proteins, contribute to upregulating Id2 expression. The synergism of the ets proteins with other transcription factors such